PHOTOCHEMICAL SYNTHESIS AND CHARACTERIZATION OF MONO- AND BI-NUCLEAR TUNGSTEN TETRACARBONYL COMPLEXES OF 2,2'-BIQUINOLINE AND 2,3-BIS(2-PYRIDYL)PYRAZINE

By

P.L. Musetha (BSc. Honours)

Submitted to the Faculty of Science and Agriculture in partial fulfilment of the requirements for the award of the degree of Masters of Science in the Department of Chemistry at the University of Zululand.

Supervisor: Professor G. A. Kolawole

(Dr N.Long supervised this work while at the Imperial College, London)

April 2002

DECLARATION

" I declare that the work described in this dissertation was carried out in the Department of Chemistry at the University of Zululand, South Africa and Imperial College of Science, Technology and Medicine, United Kingdom. All the work is my own unless otherwise stated to the contrary and has not been submitted previously for a degree at this or any other University".

MUSETHA P. L.

Table of contents

LIST OF TABLES

LIST OF FIGURES

LIST OF ABREVIATIONS AND SYMBOLS

CO	Carbon monoxide
THF	Tetrahydrofuran
MLCT	Metal-to-ligand-charge-transfer
MMCT	Metal-to-metal-charge-transfer
LF	Ligand field
Bpp	2,3-bis(2-pyridyl)pyrazine
Bppm	tetracarbonyl-2,3-bis(2- pyridyl) pyrazine.
Bqn	2,2`-biquinoline
Bpy	2,2`-bipyridine
Bpym	2,2`-bipyrimidine
Bpe	trans-1,2-bis(4-pyridyl)ethylene
Bpa	1,2-bis(4-pyridyl)ethane
Bpdz	3,3`-bipyridazine
Bpz	2,2`-bipyrazine
Bpm	4,4`-bipyrimidine
Pyz	Pyrazine
IR	Infrared
MS	Mass spectroscopy
UV	Ultraviolet
Tlc	Thin layer chromatography

CV	Cyclic Voltammetry
PL	Photoluminescence
ν	Frequency
δ	Chemical shift
TMS	Tetramethylsilane
KBr	Potassium bromide

Symbols

For IR spectral data

s	strong
vs	very strong
w	weak
m	medium

For NMR spectral data

s	singlet
m	multiplet
t	triplet

Abstract

The mononuclear and binuclear complexes of the type $[W(CO)_4L]$ and $[\{W(CO)_4\}_2]L$, where L= 2,3-bis(2-pyridyl)pyrazine(BPP), 2,2`-biquinoline(BQN), 2,2`-bipyrimidine(BPYM), and 2,2`-bipyidine(BPY), have been synthesized by direct photolysis of the metal hexacarbonyl and indirect route *via* THF substitution. In the second method, tungsten hexacarbonyl was first irradiated in THF to yield $[W(CO)_5THF]$ and the THF was then replaced by the desired ligand.

All complexes were characterised by a combination of infrared, UV-visible, ^1H NMR, mass spectroscopy and elemental analysis. Infrared spectra indicate that the complexes have approximately C_{2v} local symmetry. The absorption spectra of the complexes show intraligand band in the UV region and a broad metal-to-ligand charge-transfer (MLCT). The latter bands are red-shifted in the binuclear complexes. For comparison purposes, the properties of free ligands have also been studied. The complexes have electronic spectra dominated by intense MLCT transition in the visible region of the spectrum.

ACKNOWLEDGEMENTS

I am grateful to Professor G.A. Kolawole, my Supervisor], and Dr. N. Long who supervised the work while I visited Imperial College, London for their constant and unwavering support throughout my study. Their invaluable advice, motivation and guidance are highly appreciated. I would also like to thank Prof. P. O`Brien for funding my stay in the UK. I also thank the technical staff at the University of Zululand and Imperial College for being unfailing positive and for keeping the spirit high. Thanks are also due to the late Dr Chapman, Dr Revaprasadu, Dr Radhakrishnan , Mr Moloto and Mr Sinuka at the University of Zululand for their encouragement. Anna, from Physics is thanked for her assistance with UV-Vis spectral and photoluminiscence measurements. I would like to thank the National Research Foundation (S.A) and the Royal Society (UK) for grants supporting my work at UNIZUL . I wish to express my gratitude to my parents and my wife, Elelwani, for all the support, encouragement and patience that kept me strong throughout. I dedicate this work especially to them. Most importantly I thank God for all His mercies and kindness throughout my life.

CHAPTER 1

1.1 INTRODUCTION

1.1.1 Background

Photochemistry can be used to prepare a number of conjugated organometallic complexes selectively, efficiently and in high yield. Photochemical techniques also offer routes to highly strained compounds whose thermodynamic instability disfavours thermal methods, thus offering a simple route to organometallic compounds which overcome large enthalpy barriers and avoid high temperature conditions. The photochemical reactions are usually carried out at room temperature or below, high temperatures are unsuitable as they may lead to the decomposition of unstable ligands, complexes and reaction intermediates[1-4]. Photochemistry uses light energy to break the weakest bond in a complex and so allows substitution reactions at the metal centre to occur. For transition metal carbonyl complexes it is the metal-carbon bond that is generally cleaved. This photolysis releases a carbonyl ligand and so allows an incoming ligand to bond to the vacant coordination site on the metal.

Loss of a carbonyl ligand on irradiation is due to promotion of an electron from a metal-carbonyl bonding orbital to a strongly antibonding orbital also situated between metal and ligand. Therefore the metal-carbonyl bond is greatly weakened and carbon monoxide is lost. As the metal centre becomes more highly substituted the quantum yield of carbon monoxide loss generally decreases and eventually becomes non-observable[1-2, 5, 6-7] .That is, as the CO molecules are progressively replaced, the bonding between the metal and the remaining CO ligands becomes stronger. In some cases the substitution is carried out via a solvent-substituted intermediate. The complex may first be irradiated in a weakly coordinating solvent such as acetone, acetonitrile, pyridine, dimethylsulfoxide or, most commonly, tetrahydrofuran to yield a solvent substituted complex. The solvent molecule may then be replaced by the desired ligand at room temperature or just above. High temperatures are not needed as the solvent molecules are only weakly co-ordinated. This technique is useful if the ligand itself is photoactive, and hence damage to the integrity of the ligand could occur on irradiation[8].

1.1.2 Applications of organometallic complexes

The preparation and physical studies of N-bridged conjugated organometallic complexes and polymers have been the subject of significant research activity[2] because of the possible applications of these

compounds in the materials industry. Their photochemical and electronic properties and potential for industrial application have led to many studies. Such transition metal complexes have been of interest as potential catalysts for photo-dissociation of water by visible light, photosensitizers and conducting co-ordination polymers[16]. It is known that low-lying charge-transfer, (MLCT) transition dominates the photochemical properties of these transition metal complexes, with excited states that have been extensively investigated[5,9-15,17-19]. The unusual properties of the luminescent *tris*-bipyridine ruthenium (II) ion, $[Ru(bpy)_3]^{2+}$, as a sensitiser for the photochemical cleavage of H_2O and solar energy conversion, has lead to a vast investigation of its luminescence and redox behaviour[20,21]. Chiral bidentate ligands with C_2-symmetry play an important role in homogeneous catalytic asymmetric reaction[22].

1.1.3 Electrochemical properties of metal complexes

Attention has also been given to the electronic interaction across the ligands that bridge the binuclear complexes. On photo-excitation they provide a relatively simple route for the study and understanding of intramolecular electron transfer processes, magnetic coupling interaction from one metal to another and inner sphere electron transfer mechanisms[23-28]. The system is made up of three components:

(i) A highly absorbing (antenna) metal centre that absorbs visible light but is photochemically unreactive.

(ii) A second metal centre which undergoes a useful chemical reaction from a non-spectroscopic excited state; and

(iii) A bridging ligand which couples the two metal fragments and facilitates intramolecular energy transfer from the antenna to the reactive fragment[27].

These interactions can be varied using different ligands that will change metal-metal distance, the extent of conjugation between metal sites, complex planarity and pi-acceptor/donor ligand interaction. The electronic interaction across bridging ligand provides a simple route to the study of intramolecular electron transfer mechanism, magnetic coupling and inner-sphere electron transfer within the metal centres[30]. It is of fundamental importance to understand the role of the bridging ligand and how it can modify or control the interaction. It has been demonstrated that upon light absorption by one chromophore, these binuclear systems may undergo intramolecular energy transfer or inner sphere electron transfer, to the other chromophores. Binuclear systems are particularly interesting in that electron transfer can be studied between one metal centre and another across a conjugated system. Most of the studies of such complexes involve metals with different oxidation states. Bridged complexes of the type $(OC)_5M\text{-}L\text{-}M'(CO)_5$ and $(OC)_4M\text{-}L\text{-}M'(CO)_4$ have been synthesised[31] where M, M'= Cr, Mo, or W. The attempt to understand their photophysical

and photochemical changes that occur when forming these binulear compounds and the effect of changing the shape and degree of conjugation of the binucleating ligand between the metal centres has not been fully investigated. Creutz and Taube first reported[16] the synthesis of the complex Ru(II)-L-Ru(III) where the ligand acts as a bridge between the two metal centres in which electron transfer can take place via an innersphere mechanism. Such dimer have been synthesised by variety of routes in attempts to further elucidate the mechanism of electron transfer. Work on these ligand bridged systems using tungsten in heteronuclear complexes has been reported[16,31].

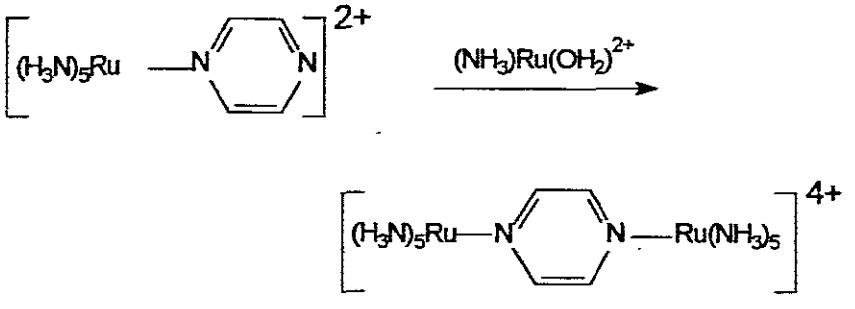

Figure 1.1: Binuclear ruthenium complex of pyrazine ligand

These binuclear metal complexes are interesting in that they are isoelectronic with the well known bridged $[(H_3N)_5Ru(Pyz)Ru(NH_3)_5]^{4+}$ complexes synthesized by Creutz and Taube[16]. Binuclear complexes were also formed by photolysis using UV light to generate a reactive THF adduct in hexane by an S_N^1 substitution reaction whereupon the THF moiety was

easily displaced by a pyridine derivative to form a bridged binuclear complex[32,33].

These compounds were found to be stable in the solid form, but in solution, are air and light sensitive. The photochemistry of unsaturated, nitrogen-coordinated, heterocyclic complexes of ruthenium (II) has been extensively studied[27]. These complexes display intense metal-to-ligand charge transfer (MLCT) bands in the visible spectral region, and therefore, have the potential for the generation of chemical potential energy from the absorption of sunlight[26-29]. To convert the radiant energy into usable chemical potential energy, the absorbing molecule must either undergo direction reaction or transfer its energy or an electron, to a second reacting molecule. Malouf and Ford[26,34] have demonstrated that $NH_3)_5Ru^{II}L$ complexes (L = substituted pyridine or pyrazine) display MLCT maxima sensitive to ligand. The two binulear complexes studied in their work are the pyrazine and 4-cyanopyridine Ru(II)-Rh(III) bridged dimers. The former complex has an MLCT maximum at 528 nm (1.89 μm^{-1}) while the same band for the latter complex occurs at 488 nm (2.05 μm^{-1}).

1.1.4 Bonding interactions of carbon monoxide with transition metals.

Low-lying unoccupied π molecular orbitals (π^*) are essential for many physical and chemical characteristics of conjugated π systems and their

complexes. Electron uptake in the ground state (reduction) or excitations to $\pi \rightarrow \pi^*$, $n \rightarrow \pi^*$ or $d_\pi \rightarrow \pi^*$ charge-transfer excited state involve at least a temporary occupation of such orbitals, their nature determining the structure and reactivity of the corresponding states [35].

Carbon monoxide has a filled σ orbital and two filled orbitals localised mainly between carbon and oxygen. Carbon monoxide is therefore classified as a σ-donor-π-acceptor ligand. It also possesses two lone pairs of electrons, localised on the carbon and oxygen atoms but directed away from the molecule. Because of the electronegativity difference between carbon and oxygen, the spatial extent of the carbon lone pair is greater than that of the oxygen lone pair. Carbon monoxide also possesses two mutually perpendicular π-antibonding(π^*) orbitals directed away from the CO internuclear region, and these two orbitals are empty in the ground state. Since oxygen is more electronegative than carbon, the filled orbitals are localized to a greater extent on oxygen than on carbon and the empty π^* orbitals are more localized on carbon. The net effect of the bonding is that carbon monoxide donates some electron density to the metal in a σ fashion from its carbon lone pair and accepts electron density from the metal in a π fashion into its π^* orbitals. Carbon monoxide is therefore classified as a σ-donor-π-acceptor ligand. It is the σ bonding, which contributes principally to the total bond energy, but the π bonding has important ramifications. Both interactions weaken the carbon-oxygen bond, although the π

interaction has the greater effect because it directly populates a C-O antibonding orbital. It is the ability of carbon monoxide to accept electron density from the metal, which allows it to stabilise metals in low oxidation states. When the ligand acts as a π-electron donor, the ligand field splitting parameter is decreased and when the ligand acts as a π-electron acceptor, the parameter is increased [2,5].

1.1.5 Infrared spectra of substituted metal carbonyls

In the past the number of observed carbonyl frequencies often has been used to help in inferring the geometries of metal carbonyls. Systematic attempts to identify the different vibrations, however, are almost restricted to studies of parent carbonyls of high symmetry, for example the hexacarbonyls $Cr(CO)_6$, $Mo(CO)_6$ and $W(CO)_6$. The C-O stretching frequencies of metal carbonyls decrease as the extent of π-electron donation from the metal to the carbonyl group increases. The steady fall of the carbonyl frequency along the series $Ni(CO)_4$, $[Co(CO)_4]^-$, $[Fe(CO)_4]^{2-}$ is a typical example of this effect[29].

Reduction of infrared active bands can be used to distinguish the CO stretching motions from the M-C stretches and M-C-O bands due to the large energy separation in these vibrations. The CO stretches generally

occur at around 2000 cm^{-1} whereas the M-C stretches and M-C-O bands are observed between 300 and 700 cm^{-1} [22,36,37].

The regular octahedral hexacarbonyls of chromium, molybdenum, and tungsten each has three carbonyl stretching vibrations of symmetries A_{1g}, E_g (doubly degenerate), and T_{1u} (triply degenerate). Only the last (T_{1u} symmetry) is active in the infrared, although the frequencies of the others can be determined from the Raman spectrum [29].

Carbon monoxide stretching frequencies of the carbonyl complexes depend on the number of CO neighbours in the complex. The stretching frequency of carbon monoxide molecule is 2168 cm^{-1}. The C-O bond order is slightly lower when the CO molecule is coordinated to a metal atom, consequently, the stretching frequency for such a CO group lies in a slightly lower frequency range, 2000 to 2100 cm^{-1}.

A bridging CO molecule, i.e. one, which is bonded to two different metal atoms, is analogous to a keto group. Because the the C-O band order in a keto group is less than that in CO, it is expected that the ketonic frequencies lie in a lower frequency range, 1700 to 1800 cm^{-1} [38]. In the IR spectra of the separated products one can observe clearly the single main peaks of the different carbonyl species.

The observed frequencies are given in Table 1.1

Table 1.1: Vibrational frequencies of metal hexacarbonyls

	Cr	Mo	W
A_{1g}^{1b}	2062.8	2119.1	2121.3
E_g^{1b}	2020.5	2021.7	2015.2
T_{1u}^{1a}	2000	2000	-

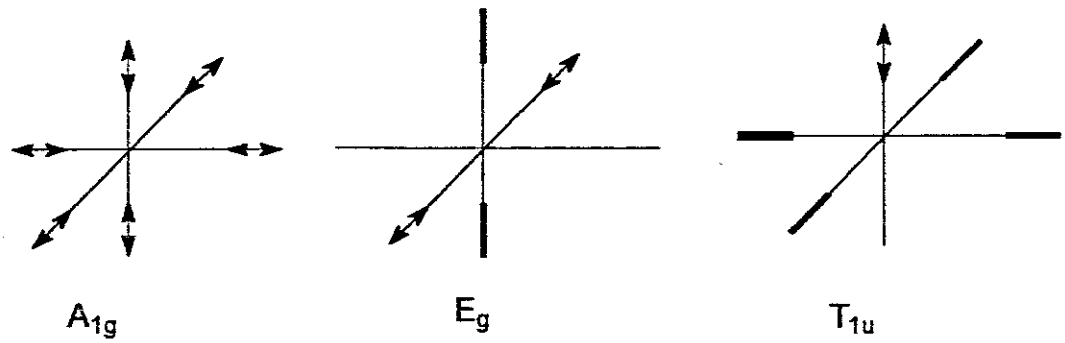

Fig. 1.2_ The carbonyl stretching vibrations of $M(CO)_6$ molecule

Stereospecifically labeled derivatives *cis*-$M(CO)_4(^{13}CO)$(amine) can arise in total or in part from a facile rearrangement of C_{4V} isomeric form of the $[M(CO)_4$(amine)] intermediate to its C_s form prior to recombination with CO[39].

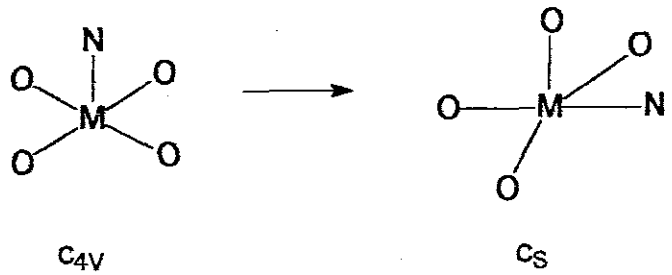

Figure 1.3_ Rearrangement of C_{4V} and C_s symmetry

Square pyramidal, coordinatively unsaturated $[M(CO)_4L]$ is found to exist in two isomeric forms :

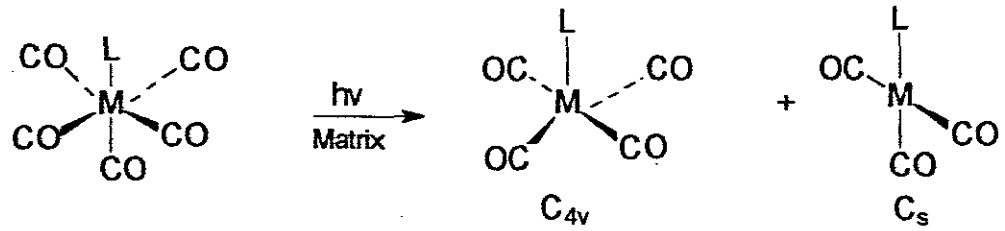

Figure 1.4_ Possible isomers of photolysis of pentacarbonyl complexes

Thus experiments suggest little selectivity in the axis of labilization. However, the lack of statistical ratio (4:1) of the C_s and C_{4v} products seemingly demands some preferential loss of axial CO, if the observed products actually are due to primary photoproducts. Study of *trans* $[(CO)W(CO)_4CS]$ revealed that the loss of CO is essentially statistical, but the primary photoproduct relaxes to a mixture of C_s and C_{4v} isomers[5].

The bands for the C_{2V} complexes are modestly red shifted from those of the C_{4V} $[M(CO)_5(amine)]$, as expected for LF bands in the $C_{4V} \rightarrow C_{2V}$ descent in

symmetry. $[M(CO)_5amine]$ compounds are ideally of C_{4v} symmetry resulting in three infrared active CO stretching vibrations, two of symmetry A_1 and one of E symmetry. These are observed at approximately 2075(w), 1935(vs), and 1920(s) cm^{-1} for $A_1^{(2)}$, E, and $A_1^{(1)}$ symmetry modes, respectively. In addition, bands of very low intensity are observed at ~2066 and 1905 cm^{-1} and are assigned to vibrations due to CO in natural abundance in one equatorial position. This has been confirmed by isotopic enrichment studies in $[Mo(CO)_5(piperidine)]$[40]. For only two types of compound are the spectra of substituted carbonyls directly comparable with those of the parent hexacarbonyl, namely, for *trans*-$[L_2M(CO)_4]$ and $[L_4M(CO)_2]$, where L is an axially symmetric ligand. In each case there is just one allowed C-O vibration of the hexacarbonyl. Apart from very small effects due to the change in the "effective mass" of the central metal ion changes in the allowed frequency in the series $M(CO)_6$, *trans*-$[L_2M(CO)_4]$, and *trans*-$[L_4M(CO)_2]$ are directly attributable to the "electronic" influence of *cis* substitution. Raman spectra for these substituted compounds would be very helpful. The infrared carbonyl stretching frequencies from the series of $[(OC)_5M(pyz)M'(CO)_5]$ and $[M(CO)_5Pyz]$ as Nujol mull also indicate that the local C_{4v} of the $M(CO)_5$ groups in $[(OC)_5M(pyz)M'(CO)_5]$ is preserved[31].

Table 1.2 Relation of the number of CO stretching bands in the IR spectrum to structure[45].

Complexes	Isomer	Structure	Point Group	Number Of Bands
$M(CO)_6$			O_h	1
$M(CO)_5L$			C_{4v}	3
$M(CO)_4L_2$	trans		D_{4h}	2
$M(CO)_4L_2$	cis		C_{2v}	4
$M(CO)_4L$	ax	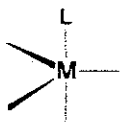	C_{3v}	3
	eq		C_{2v}	4
$M(CO)_3L_2$			D_{3h}	1
		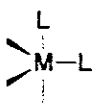	C_s	3
$M(CO)_4$			T_d	1

The complex $[Cr(CO)_4(PPh_3)_2]$ has one very strong infrared absorption band at 1889 cm^{-1} and two other very weak bands in the CO stretching region. A disubstituted hexacarbonyl may exist with either *cis* or *trans* configurations. In the *cis* isomer the four CO ligands are in low symmetry (C_{2v}) and therefore four infrared bands should be observed as indicated in Table 1.1. The fact that for the *trans* isomer only one active band is predicted whereas in the *cis* structure four bands are expected points out a

Table 1.3. CO Vibrational stretching frequencies of tetracarbonyl complexes[39].

Complex	Tetracarbonyls			
	$A_1(s)$	$B_1(vs)$	$A_1(sh)$	$B_2(s)$
$[(bpy)Mo(CO)_4]$	2010	1905	1888	1845
$[(bpdz)Cr(CO)_4]$	1998	1900	1900	1865
$[(bpdz)Mo(CO)_4]$	2001	1900	1900	1862
$[(bpdz)W(CO)_4]$	2000	1893	1893	1860
$[(bpm)Cr(CO)_4]$	2010	1905	1905	1855
$[(bpz)W(CO)_4]$	2018	1927	1905	1857

Table 1.4. Pentacarbonyls complexes[39].

Complex	Pentacarbonyls		
	A_1(w)	E(vs)	A_1(s)
[(bpdz)W(CO)$_5$	2055	1925	1895
[(bpdz){W(CO)$_5$}]$_2$	2055	1925	1895
[(bpm)W(CO)$_5$]	2070	1935	1907
[(bpm){W(CO)$_5$}]$_2$	2065	1935	1905

general rule for infrared activity:

> "the more symmetric the molecule, the fewer infrared active bands are to be expected"[36,37].

A monosubstituted metal carbonyls [LM(CO)$_5$] has symmetry C_{4v} and [L$_2$M(CO)$_4$] has a symmetry C_{2v} [29]. Formal symmetry rules show that the vibrations may be classified as shown in Figures 1.6 and 1.7.

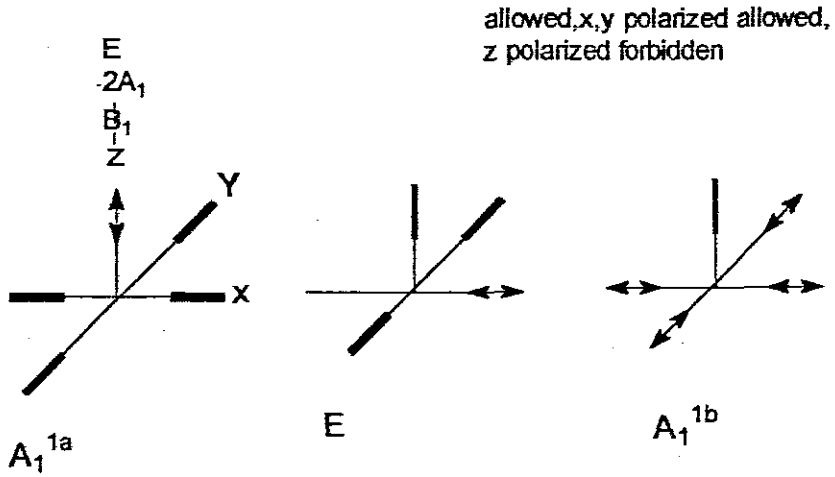

Figure 1.5_ The allowed carbonyl stretching frequencies of [LM(CO)$_5$] molecules

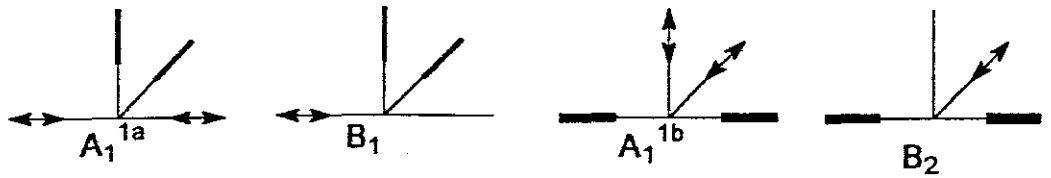

Figure 1.6_ The carbonyl stretching frequencies of cis-[L$_2$M(CO)$_4$] molecules

All the [LM(CO)$_5$] complexes have C_{4v} symmetry at least ideally, and give rise to three allowed infrared absorption (two non-degenerate and one doubly degenerate), having the symmetry labels $A_1^{(1)}$, $A_1^{(2)}$, and E.

First, the E vibration corresponds closely to the T_{1u} vibration of the parent

hexacarbonyl and should account for very roughly 4/5 of total intensity of absorption. The two A_1 vibrations are made up from the stretching mode of the unique carbonyl group and the symmetrical breathing mode of the other four. Since the two A_1 modes are of the same symmetry and similar in energy, they are strongly coupled. Symmetry forbids, however, any coupling between B_1 or B_2 with each other or with the A_1 vibrations. If these A_1 motions did not couple together the former would be allowed, accounting for the remaining 1/5 of the total intensity, while the latter would be almost forbidden (it still could have small intensity due to non-coplanarity of the radial carbonyl groups and to electronic migration along the four-fold axis accompanying the symmetrical stretching of the radial carbonyl groups). In fact the two A_1 modes interact and some of the intensity of the strongly allowed one must be transferred to the other. This elementary discussion leads us to expect a very strong band, a band which is less strong by a factor of roughly four, and a third much weaker band. The sign of the interaction constant between carbonyl groups places the weak A_1 band at a higher frequency than the E band, and analogy with the hexacarbonyls suggests that for example in molybdenum compounds there should be an interval of 100-120 cm^{-1} between them. The position of the stronger A_1 band cannot be predicted.

The *cis*-$[L_2M(CO)_4]$ compounds, having a C_{2v} symmetry, have been found to be complicated [29]. It is convenient to consider the *trans* pair of carbonyl groups first since they give rise to an antisymmetric B_1 stretching mode

corresponding to one component of the T_{1u} mode of hexacarbonyl and an almost forbidden A_1 mode. The other two carbonyls give two allowed vibrations of symmetry A_1 and B_2, which should have comparable intensities. Finally the two A_1 modes must interact. We expect, as in the pentacarbonyls, a pair of bands, one very strong and the other weak, separated by 100-120 cm^{-1}, and in addition two bands of intermediate strength. Analogous arguments show that in *cis*-dicarbonyls there should be two bands of comparable strength, while in symmetrical C_3 tricarbonyls we expect two bands, a degenerate one at lower frequency having very roughly twice the intensity of the bands separated by about 100 cm^{-1} and other moderately strong band due to the unique carbonyl group.

The spectrum of $[P(C_2H_5)_3Mo(CO)_5]$[41] is reported to consist of two peaks, at 1942 cm^{-1} and 2064 cm^{-1}, the stronger of which is composed of two close-lying but resolvable bands. *Cis*-$[P\{(C_2H_5)_3\}_2Mo(CO)_4]$ is reported[17] to have four bands at 2014± 2, 1915 ±1, 1900.5 ± 1, and 1890± cm^{-1}, but no relative intensities are quoted. Fortunately such data are available for closely related *cis*-$(P(C_6H_5)(C_2H_5)_2Mo(CO)_4]$,namely:2012 (strong); 1907 (shoulder); 1895 (very strong); 1866 (strong).

Two particularly interesting compounds with almost identical spectra are $[XMo(CO)_4]$ where X is *o*-phenanthroline or α,α′-dipyridyl. The reported bands are at 2020 (m), 1901 (vs), 1877 (s), and 1826 (s) for dipyridyl complex. The higher pair is due to the *trans* pair of carbonyls and has an appropriate separation of 104 cm^{-1}. The *cis*-carbonyl frequencies have been

depressed far more than in phosphines and have come out clear of the *trans* pair at 1877 cm^{-1} and 1826 cm^{-1}. This is in very sharp contrast with the situation in *cis*-disphosphines [41].

1.1.6 Electronic absorption spectra

Complexes of C_{2V} symmetry, $[M(CO)_4L]$ (L = bidentate ligand) or *cis*-$[M(CO)_4L_2]$, have been studied [29]. The $M(CO)_4L$ complexes exhibited low lying ligand field (LF) and varying degrees of stability in solution. In C_{2v} complexes of unsaturated nitrogen-donor ligands MLCT and IL transitions are observable. For L= pyridine, the LF and MLCT transition in *cis*-$[M(CO)_4L_2]$ are overlapping as in $[M(CO)_5L]$. But in tetracarbonyl complexes of 2,2'-bipyridine, 1,10-phenanthroline and related ligands the MLCT band system is well below the LF band system. The MLCT depends on the substituents on L in a manner consistent with the direction of the CT and as in the $[M(CO)_5L]$ complexes, the MLCT band position blue-shifted significantly from alkane to more polar or polarizable solvents. The LF band in $[M(CO)_4L]$ is still present at ~400 nm in those complexes having a lowest MLCT band. *cis*-$[W(CO)_4(trans\text{-}4\text{-}styrylpyridine)_2]$ exhibits an MLCT absorption as the lowest energy absorption and an IL transition in the near-UV region.[5]

In C_{2V} complexes of unsaturated nitrogen-donor ligand MLCT and IL transitions are observable. The removal of a CO from $[M(CO)_5]$ to generate

the C_{4V} species affect the d-orbital. The lowest energy spectral feature of $[M(CO)_5]$ has been assigned as the $^1A_1(e^4b_2^2) \rightarrow {}^1E(e^3b_2^2a_1^1)$ LF absorption and the polarisation of the band is consistent with the interpretation. The lowest energy absorption band for $[M(CO)_5]$ is significantly red shifted when compared to $[M(CO)_6]$, as expected.

Reports of ligand-bridged species bound between two $M(CO)_5$ moieties of the type $[(CO)_5M\text{-}L\text{-}M'(CO)_5]$ and between two $[M(CO)_4]$ fragments of the type $[(CO)_4M\text{-}L\text{-}M'(CO)_4]$, (where M, M' = Cr, Mo, W) have appeared [16]. These studies demonstrated that the binucleating ligand π^*-electron system has a profound effect on the spectroscopic, photochemical, and redox behaviour of these complexes.

Each complex exhibits low lying $^1A_1 \rightarrow {}^1E$ ligand field and $M \rightarrow \pi^*(L)$ charge-transfer absorptions[43]. The position of the energy of the MLCT transition is dependent on both the length and conjugation of the binucleating ligand, where L = pyz, bpy and bpe, the MLCT states are at lowest energy, but when L = bpa, the ligand field states are lowest lying. Complexes having ligands with low-lying excited states exhibit intraligand transitions. One interesting case is $[W(CO)_5$(styrylpyridine)], the complex exhibits a low lying IL ($\pi \rightarrow \pi^*$) absorption, but these are overlapping LF and MLCT bands. The intense near UV intraligand ($\pi \rightarrow \pi^*$) transition is observed near the position found in the free ligand. Overall, the MLCT energies for the ligand bridged dimers are ordered L = bpa > bpy > bpe >

pyz (indicated in Figure 1.8)[31] indicating that the energy of the ligand π*-acceptor orbital is dependent on both the length and conjugation of the binucleating ligand. Higher frequencies are found for $[Mo(CO)_4L]$ compounds with L= 2,2` bipyridine indicating the presence of π-backbonding from Mo to L [31].

Electronic absorption spectra reveal the presence of $^1A_1 \rightarrow {}^1E$ ligand field (LF) and M→π*(pyz) transitions in all species. In each case the MLCT bands are attributed to be at lowest energy; these transitions are substantially lowered in the binuclear molecules and reflect the perturbation of the pyz π*-acceptor system. The absorption spectra indicate that the chromophores`LF transitions are relatively unaffected on binucleation, whereas the energy of the ligand π* system is influenced by both metals [44].

In electronically-coupled valence-localized dimers, metal-to-metal charge-transfer, or intervalence transfer dimer absorption features

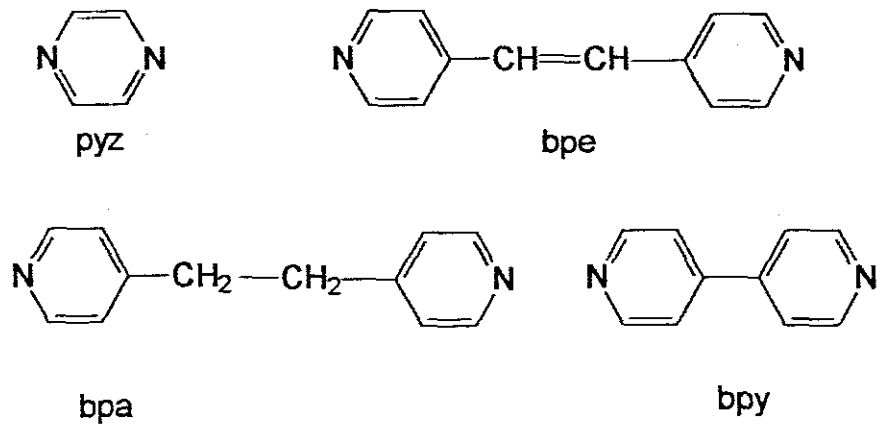

Figure 1.8. Published complexes of binucleating ligands(L) [pyrazine (pyz), 4,4-bipyridine (bpy), trans-1,2-bis(4-pyridyl)ethylene (bpe), and 1,2-bis(4-pyridyl)ethane (bpa)

may be observed that correspond to optically-induced electron transfer between the two metals. As electronic coupling is increased, the description of this absorption process evolves to one of electron promotion between bonding and antibonding (or non-bonding depending on the bridging ligation) dimer wave functions.

Table 1.5: Electron absorption spectra data[27,31].

Complex	λ_{max}/ nm
$[Cr(CO)_4(bpym)]$	499, 389
$[W(CO)_4(bpym)]$	478, 371
$[\{W(CO)_4\}_2(bpym)]$	610, 210, 385
$[Ru(NH_3)_4(bpym)]^{2+}$	567, 402
$[\{Ru(NH_3)_4\}_2(bpym)]^{4+}$	697, 428
$[\{W(CO)_5\}_2bpy]$	405, 438
$[W(CO)_5bpy]$	400, 370
$[\{W(CO)_5\}_2bpa]$	375, 347
$[\{W(CO)_5\}_2bpe]$	405, 450

Some generalities on the table can be observed. In comparing analogous monometallic and bimetallic systems e.g. $[Ru(NH_3)_4(bpym)]^{2+}$ and $[\{Ru(NH_3)_4\}_2(bpym)]^{4+}$, the bimetallic complex displays an additional band

at the low energy end of the spectrum which extends the absorption spectrum of the antenna fragment when it is bound to another metal centre. The visible absorption spectrum of $[\{(NH_3)_4Ru\}_2(bpym)]^{4+}$ exhibits two bands.

The higher energy band occurs at 428 nm (ε = 1.8 x 10^4 $m^{-1}cm^{-1}$), with a lower energy band at 697 nm (ε = 4.0 x 10^3 $m^{-1}cm^{-1}$)[14]. Owing to the similarity of peak position and intensity of the bimetallic complex to those of the corresponding monometallic complex, the more intense bimetallic band is also probably metal-to-ligand charge-transfer in character. The lower energy absorption at 697 nm is similar in position and intensity to the low energy absorption of the previously reported $[(bpy)_2Ru]_{1,2}(bpym)]^{2+,4+}$ bimetallic complex [45,46]. In both $[\{bpy)_2Ru\}_{1,2}(bpym)]^{2+,4+}$ the absorption maxima are at lower energy in comparison to those of the $[\{(bpy)_2Ru\}_{1,2}(bpym)]^{2+,4+}$ analogues. The absorption maxima for $[\{bpy)_2Ru\}_{1,2}(bpym)]^{2+,4+}$ occur at a lower energy than the corresponding $(bpy)_2$ complexes. These results are due to the ability of the bpy π^* orbitals to participate in π-backbonding with the Ru(II). This results in an additional stabilization of Ru(II) dπ orbitals. The source of this transition is outlined in Figure 1.9. The complex, $(NH_3)_5Ru^{II}$-4-cyano-pyridine-$Rh^{III}(NH_3)_5$, has an absorption maximum at 488 nm which is assigned as a MLCT from Ru(II) to 4-CNpy. [27]

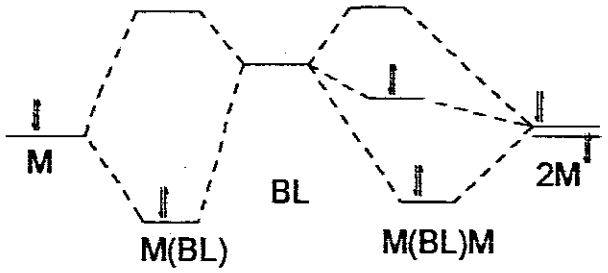

Figure 1.8: Partial molecular orbital diagram for the mononuclear and symmetrical bimetallic species[27].

In the above Figure 1.9, M is a metal and BL is a bridging ligand.

The spectra of the pentacarbonyl compounds are remarkably similar, as expected, when considering that the heterocyclic ligand system in [{$W(CO)_5$}$_2$bpa] is unconjugated beyond the pyridine rings. In most of the compound, the charge transfer transition ($\pi^* \leftarrow {}^1A$) occurs at higher energy than the ligand field band, and the ligand field band is solvent insensitive. In the compound [$W(CO)_5$bpy], the charge-transfer transition has moved to lower energy than that for $W(CO)_5]_2$bpa, and in fact it is observable only as a shoulder (more discernible in acetone) on the high energy side of the ligand field band. The lowest energy transition in the electronic absorption spectra of [$M(CO)_5$(4,4`-bipy)] and [$M(CO)_4$-(4,4`-bipy)$_2$], is substantially red-shifted by formation of the oligomers, consistent with the assignment of

this feature as a metal to ligand charge transfer transition. The fact that the transition moves significantly on formation of the oligomers suggests that the energy of the π*-acceptor orbitals on the 4,4`-bipy ligand are effectively lowered on association of the monomers to form oligomers. The peaks observed in the oligomers at between 395 nm and 415 nm are attributed to ligand field transitions[4]. These are not shifted significantly from those observed in the monomers. The π-π* ligand-ligand transitions of 4,4`-bipy, observed at ~247 nm in the monomers, are essentially unaffected by formation of the oligomers[2, 4,46-48,59].

1.1.7 Solvents effect on organometallic complexes

A combination of spectroscopic, photochemical, and electrochemical techniques has been used to investigate solvent effects on the excited states and deactivation parameters of binuclear complexes and their corresponding mononuclear derivatives.

Ligand bridged $[(CO)_5W\text{-}L\text{-}W(CO)_5]$ complexes exhibit a strong negative solvatochromism associated with the MLCT transitions whereas the ligand field transitions are relatively unaffected. This solvent dependence arises from specific solvent-solute and induced dipolar interactions in addition to changes in metal-ligand bond polarity during the MLCT transition. Dual MLCT emission bands have been observed, but lifetime data reveal that these MLCT states are thermally equilibrated [42]. Emission spectra exhibit

solvent shifts in the direction opposite to that for absorption spectra, and this effect is rationalised on the basis of a scheme that depicts a contraction of the W-N bond in the excited state relative to the ground state geometry. Solvent predominantly affects the non-radiative decay rates, in some cases Knr data illustrate an energy gap. Solvent effects on redox potential data substantiate the HOMO/LUMO assignments and further indicate the extent of Franck-Condon perturbation. On photolysis the complexes undergo W-N bond dissociation. Effects of solvent on this reaction efficiency are small and are incorporated in the excited state model[38,49].

Solvent sensitivity in these complexes is profoundly dependent on the electronic characteristics of the ligand and the extent that the ligand π^* orbitals are mixed with metal $d\pi$ character. The MLCT transition in these binuclear complexes actually comprises two orbital allowed components, although these states are thermally equilibrated at room temperature. The two MLCT transitions have widely differing solvent sensitivities. Solvent effects on photophysical and photochemical parameters are predominantly influenced by changes in Knr values. There is some basis for interpreting this via an energy gap law relationship, but specific and induced solvent dipolar interactions must be also invoked in the excited-state degradation mechanism[31,43,49].

In a nonpolar solvent, the MLCT absorption further red shifted and exhibits the features of two components [34, 38].

1.1.8 Photosubstitution of metal carbonyl complexes.

The synthesis of mononuclear and binuclear organometallic complexes linked by conjugated N-containing heterocycles is of interest [51,53].

The ligand photosubstitution chemistry of $[M(CO)_5L]$ complexes, were M = Mo or W and L = amine has been demonstrated to involve both CO and L substitution via dissociative mechanism with M-L cleavage (1.1) and not M-CO cleavage (1.3) being dominated[11,53,59,61]. Photochemical path ways are :

$$M(CO)_5L + CO \rightarrow M(CO)_6 + L \qquad (1.1)$$

$$M(CO)_5L \rightarrow M(CO)_5L' + L \qquad (1.2)$$

$$M(CO)_5L \rightarrow M(CO)_4LL' + CO \qquad (1.3)$$

The pathways are dependent on the wavelength of irradiation, the metal and the ligand L. A higher quantum yield of CO ejection was found after short wavelength irradiation and /or in going from M = W to Mo and Cr[6,39]. A drastic reduction of quantum efficiency is found when MLCT transition is lowest in energy for ligands having low-lying π^* orbitals. For the photochemical process (1.2) the total reaction quantum yield was less than unity, showing that radiative and nonradiative deactivation processes must be involved. The quantum yields of both reactions are dependent on the

wavelength, e.g. reaction 1.3 is dominant at long wavelengths, whereas reaction 1.4 becomes increasingly important at shorter wavelength.

Indirect and direct methods have been used to synthesise different complexes. First, $[M(CO)_5pyz]$, M= Cr, Mo, W were synthesised via corresponding tetrahydrofuran complex, $[M(CO)_5THF]$ (reaction 1.4 and 1.5)

$$M(CO)_6 \xrightarrow[\text{Ar-purged THF}]{h\nu,\ 313\ nm} [M(CO)_5THF] + CO \quad ---(1.4)$$

$$M(CO)_5THF \xrightarrow[Pyz]{} [M(CO)_5pyz] + THF \quad --- \quad (1.5)$$

The $[M(CO)_5pyz]$ complexes were subsequently thermal reacted with photochemically generated $[M'(CO)_5THF]$ (reaction 1.6 and 1.7).

$$[M'(CO)_6] \xrightarrow[\text{Ar-purged hexane+ 0.1MTHF}]{h\nu,\ 313\ nm} [M'(CO)_5THF] + CO---(1.6)$$

$$M'(CO)_5THF \xrightarrow[M(CO)_5pyz]{} [(OC)_5M(pyz)M'(CO)_5] + THF \quad --- \quad (1.7)$$

Reaction 1.7 was carried out in hexane containing 0.1M THF, rather than THF, to avoid thermal decomposition of $[(OC)_5M(pyz)M'(CO)_5]$, which occurs in polar solutions. In hexane the binuclear products are virtually insoluble and precipitate out of solution.

An alternative route was found to yield the $[(OC)_5M(pyz)M'(CO)_5]$, complexes, where M = M' (reaction 1.8).

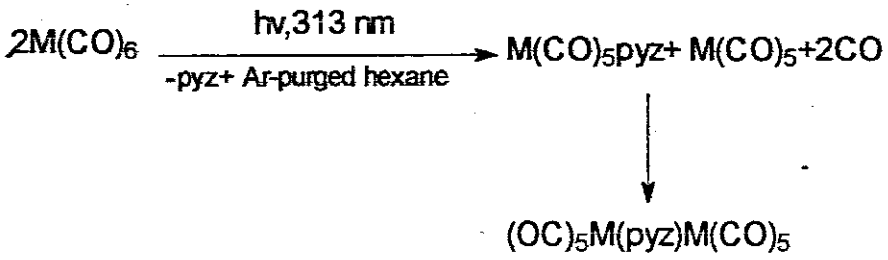

The initial photoproducts, $M(CO)_5pyz$ and $M(CO)_5$, immediately combine to form $[(OC)_5M(pyz)M(CO)_5]$, which precipitates out of solution. The formation of $[M(CO)_5pyz]$ during the reaction was confirmed by UV-visible spectroscopy. The other primary photoproduct is presumably unsaturated $[M(CO)_5]$ which reacts rapidly with $[M(CO)_5pyz]$ to form the binuclear product.

1.1.9 Photochemistry of tetracarbonyl and pentacarbonyl complexes

Metallorganic dimers have been synthesised by a variety of routes in attempts to further elucidate the mechanism of electron transfer[54]. These complexes were found to be stable in solid form, but in solution are air and /or light sensitive. The instability of these complexes is thought to be due to cleavage of the M-L-M bond as shown in the bridged dimer $[(OC)_5Mo(pyz)Mo(CO)_5]$. Binuclear 4,4'-bipyridine systems have also been synthesised and show similar light- and air-sensitivity. Depending on the UV-lamp and solvent, different products from the same ligand were reported[2].

Consider irradiation of dichloromethane solution of $[M(CO)_6]$ (M = Cr, Mo, W) and the ditopic, non-chelating ligand 4,4`-bipyridine in a 1:2 ratio leads to the *cis* substituted complex $[M(CO)_4(4,4`\text{-bipy})_2]$ in 95% yield.

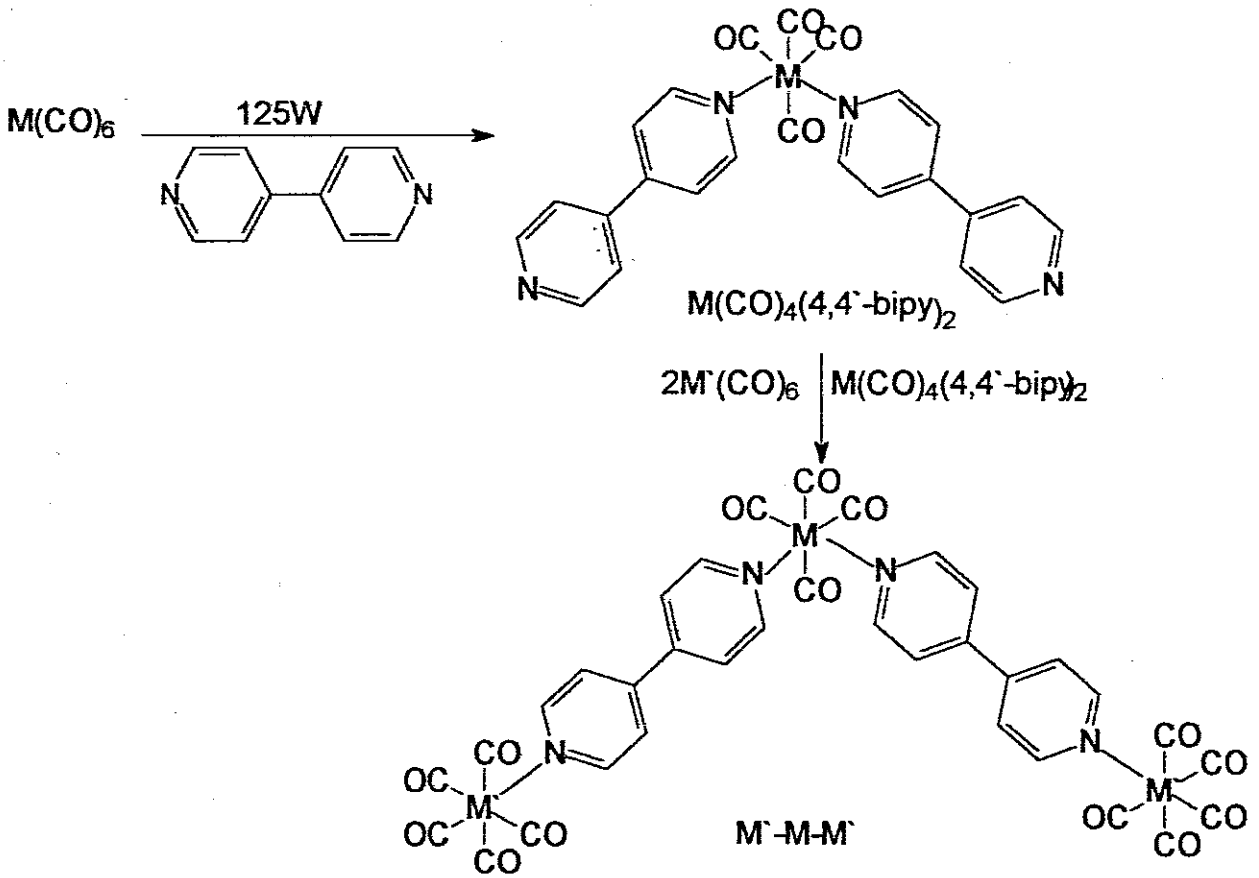

Figure 1.9 4,4`-Bipyridine photoproducts existing as tetracarbonyls

Subsequent photolysis of $[M`(CO)_6]$ (M = Cr, Mo, W) and in 2:1 ratio leads to the formation of the homometallic or heterometallic or trimetallic

complexes [(CO)$_5$M`(4,4`-bipy)M(CO)$_4$(4,4`-bipy)M`(CO)$_5$,denoted as M`-M-M`, in between 75 and 85% yield[2].

Irradiation of dichloromethane solution of [M(CO)$_6$] and the ligand 4,4`-bipyridine in either 1:1 or 2:1 ratio, respectively yield pentacarbonyl complexes.

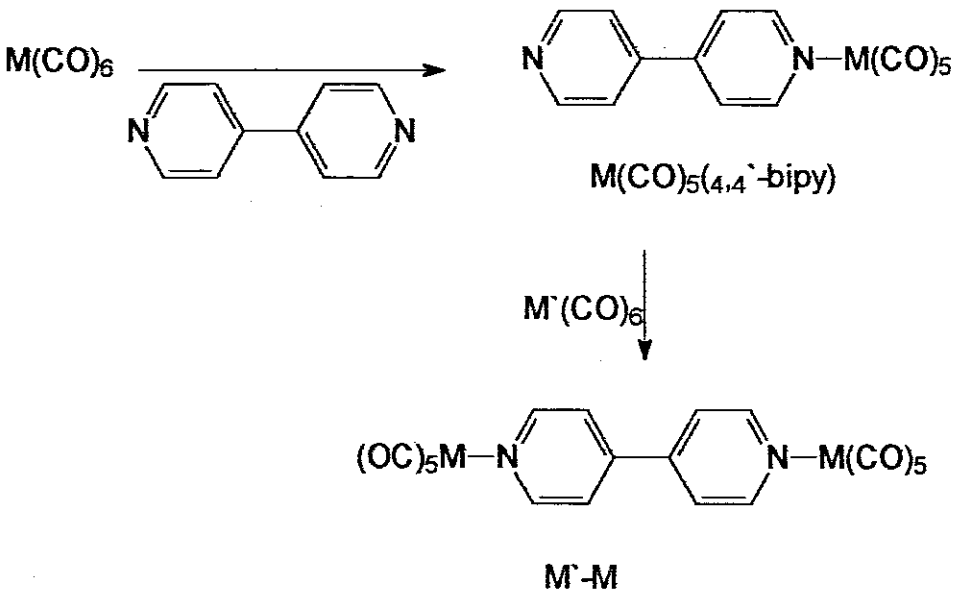

Figure 1.10_ 4,4`-bipyridine photoproducts existing as pentacarbonyls

These complexes can be prepared by direct photolysis at λ=313 nm of two moles of tungsten hexacarbonyl with one mole of 4,4`-bipyridine in hexane at room temperature yielding a mixture of both monomeric and dimeric complexes[51].

1.1.10 Luminescence Studies

Only a few luminescent Cr, Mo, or W carbonyls are known. The first reports of luminescence from any metal carbonyl involved C_{4V} complexes of the general formula $[W(CO)_5(N\text{-electron donor})]$. Emission was observed at 77 °K in solution or the pure solid.[1]

Absorption and emission spectral studies of $[M(CO)_4L]$ complexes (M = Cr, Mo, W, L= 2,2`-bipyridine, 1.10-phenanthroline, 5-CH_3, 5-NO_2-1,10-phenanthroline) have been carried out and reveal that the lowest excited state in every case is charge-transfer in character, MLCT in absorption, and in no case do the ligand field excited states cross below the CT state. For the $[M(CO)_4L]$ complexes, emission is detectable for M = Mo or W and occurs in the range 14.40-15.66 kK with lifetimes of 7.9-13.3 microsec and quantum yields of 0,02-0.09. A qualitative report of the electronic emission of the bipy and several methyl-substituted bipy complexes suggests that the lowest excited state emission is also CT in character. For the $[M(CO)_6]$ and $[M(CO)_5X]$, (X = N-electron donor) complexes the low energy absorption shoulder present only for M = W has been ascribed to a spin-forbidden ligand field transition. Ligand field and MLCT states are also emissive at low temperature for the C_{2v}. The low energy shoulder in the $[W(CO)_4L]$ complexes was assigned to a singlet→triplet MLCT absorption[56,59,61].

The observation of optical emission at 298 K is significant in that the $[W(CO)_5X]$, (X = N-electron donor) complexes which exhibit ligand field

The observation of optical emission at 298 K is significant in that the $[W(CO)_5X]$, (X = N-electron donor) complexes which exhibit ligand field luminescence only emit at low temperature. Emission from $[M(CO)_4L]$ complexes is also in contrast to the $[M(CO)_5X]$ since for the C_{4v} complexes only the W complexes are luminescent[42]. Several complexes of the general formula $[W(CO)_5L]$, where L is an N-electron donor, have been found to luminesce at 77 K either as the pure solid or in rigid glasses. The emission has been assigned to either a $^3E \rightarrow {}^1A_1$ ligand field transition or a $W \rightarrow L$ charge-transfer transition, depending on the nature of the ligand. As ligand becomes more electron withdrawing, the CT state lowers in energy and for various 4-substituted pyridines as L has been inferred to be the lowest lying state. The $[(OC)_5M(pyz)M'(CO)_5]$ complexes, each complex exhibit broad, unstructured emission in the 550-800 nm region[29].

Table 1.6 Emission spectral data of $[(OC)_5M(pyz)M'(CO)_5]$ in benzene at 283 K[29].

Complex, M, M'	Maxima, nm
Cr, Cr	702
Cr, Mo	687
Mo,Mo	675
Mo,W	712
W,W	722
W,Cr	707

The onset of emission in the 550-600 nm region leads us to assign the emission of each complex to the lowest energy M→ π*(pyz) excited state. The emission is assigned to a lower energy MLCT component. This is analogous to the MLCT emission that has previously been observed from $[M(CO)_5L]$ and *cis*-$[M(CO)_4L_2]$ complexes where M = Cr, Mo, W and L = a pyrazine derivative. Each of the complexes gives rise to a single broad emission band in the 500-750 nm region, the emisssion is assigned to the lowest energy M→ π*(L) MLCT excited state, as previously noted for $[(OC)_5W(pyz)W(CO)_5]$ and several mononuclear group pentacarbonyl derivatives. When L = bpy and bpe, the emission maxima of the ligand-bridged dimer complexes are only slightly red shifted than that for the $[(OC)_5W(pyz)]$ complex [55,61-64].

1.1.11 Electrochemistry of organometallic complexes

Cyclic Voltammograms have been recorded on a number of the monometallic and bimetallic systems. The information obtained from these studies indicates the degree of communication possible between the antenna and reactive fragment mediated by the bridging ligand[25,33,37,63]. Table 1.7 summarises these data. In all cases, for both monometallic and bimetallic system, M(III)/M(II) reduction potentials are more positive for bpym complexes than the analogous bpy complexes. This observation is

consistent with the better π-acceptor ability of bpym .vs bpy and is manifested in the lower energy electronic transition for the bpym analogue as well. The cyclic voltammogramms of the mixed- ligand complexes of Fe(II) with CN^- and bpym show an increasing Fe(III)/Fe(II) reduction potential as more bpym ligands appear in the coordination sphere. In the Ru(II) complexes, the same type of behaviour is observed for the RuL_4(bpym) complexes. The greater the π-acceptor ability of the L_4 ligands, the more positive the Ru(III)/Ru(II) couple[32,33,54-56,61,65].

Table 1.7: Redox Potentials of bidiazine ligands and their carbonyl metal complexes[39].

Complex	E_{ox}(+/0)	E_{red}(0/-)	E_{red}(-/2-)
[(bpy)Mo(CO)$_4$]	+0.82	-1.40	-2.15
[(bpym)Mo(CO)$_4$]	+0.84	-1.07	-1.71
[(bpdz)W(CO)$_4$]	+0.70	-1.04	-1.85
[(bpdz)[W(CO)$_5$]$_2$	+1.02	-0.90	
[(bpm)W(CO)$_4$]	+0.86	-0.68	-1.39
[(bpm){W(CO)$_5$]$_2$	+1.01	-0.67	-1.35

1.1.12 X-ray crystallography

Single crystal X-ray diffraction provides a unique insight into the overall assembly of the atoms within a complex, the success of this technique is totally dependent upon the growth of single crystals of suitable quality. This technique is also useful in determining the absolute configuration of complexes of optically active ligands. The structures of 2,2′-bipyridine **(1)** and 2,2′-bipyrimidine **(2)** complexes were determined by single X-ray diffraction methods[66]. Complex **(1)** has C_{2v} symmetry about an axis passing through the tungsten centre and bisecting the bond between the two aromatic rings. The tungsten is coordinated to both ring nitrogen atoms, two axial and four equatorial CO groups in a distorted octahedral geometry. Notably the two axial carbonyl ligands are bent away from the bipyridine unit (<C(15)-W-C(16) = $167.9(13)^0$. The molecules formed stepped stacks with the N(1) containing pyridyl ring of one molecule overlaying the M(8) containing ring of the next and so on(F1b).

Complex **(2)** coordinates at N(1) and N(3), leaving N(2) and N(4) free (figure 2). It also has molecular C_{2v} symmetry about the axis passing through the tungsten centre and bisecting the bond between the two aromatic rings. The octahedral geometry is also distorted, with *cis* angles in the range $72.31(18)$-$100.0(3).^0$ The most acute angle, associated with the bite of the chelating ligand (due to orbital repulsion effect), is observed. Reaction schemes of the complexes of two ligands are shown below:

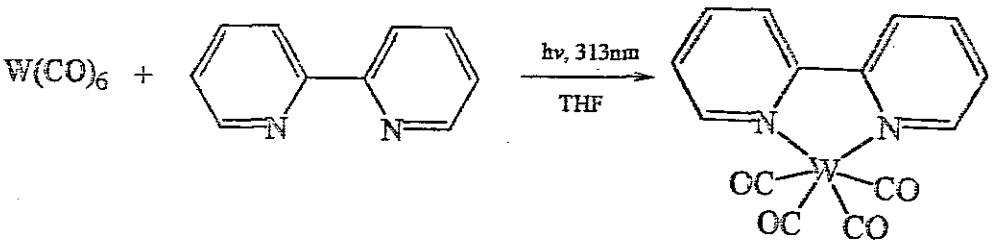
W(CO)6 +
hν, 313nm
THF
N
N
N
N
W
OC
CO
OC
CO

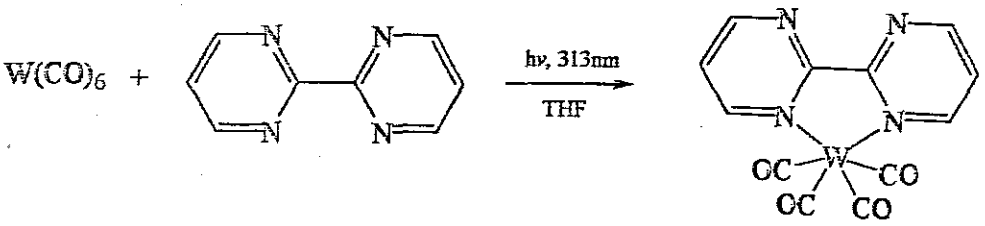
W(CO)6 +
hν, 313nm
THF
N
N
N
N
N
N
W
OC
CO
OC
CO

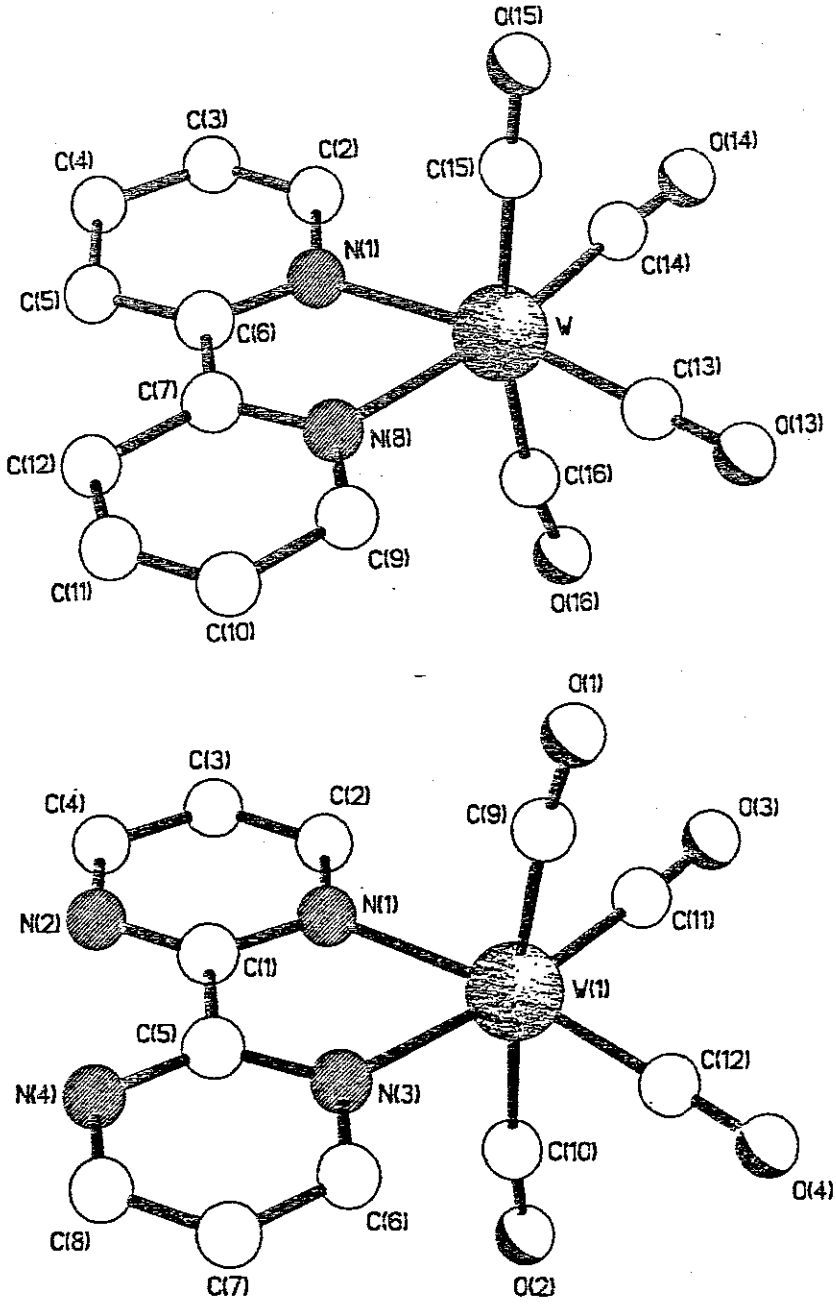

Figure 1.11 _ X-ray structure of $[W(CO)_4bpy]$ and $[W(CO)_4bpym]$

1.1.13 The rationale and objectives of this study

Following the synthesis of the mono- and bi-nuclear complexes of the type $[W(CO)_4L]$ and $[\{W(CO)_4\}_2L]$ where L= 2,2′-biquinoline , 2,3-bis(2-pyridyl)pyrazine, 2,2`-bipyrimidine and 2,2`-bipyridine, the isolated compounds have to be fully characterised by chemical and spectroscopic techniques. 2,2`-Bipyrimidine and 2,2`-bipridine were prepared using THF (indirect method) as a solvent. New method has been employed for comparison, and it was found to be more effective than the earlier method. Direct photolysis was used to prepare the complexes because the earlier method require many reactions to gradually build up the structure and so is a slow process which lead to a reduced yield at each step. Some of the reactions lead to unwanted/side products, which make separation difficult. The latter method is reasonably fast and gives high yield. Only the monomer for bipyrimidine has been prepared before, so with the latter method the monometallic complexes could then be transformed to bimetallic complexes in order to investigate the electron interaction between the two metal centres. Bipyrimidine ligand has been repeated due to the fact that it is unique among the bidiazine (4-N) isomers by the possibility of forming binuclear complex on the second co-ordination. The ^1H NMR, Cyclic voltammetry, photoluminescence, and UV-visible have not been done before, so there is still a need to characterise them.

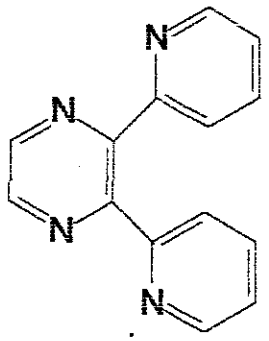

2,3-bis(2-pyridyl)pyrazine (BPP)

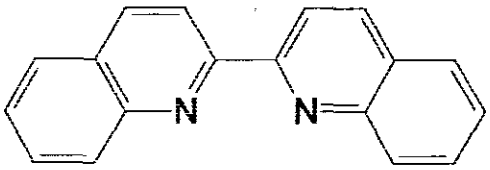

2,2`-biquinoline (BQN)

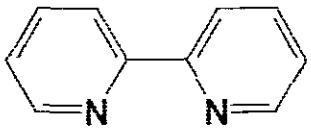

2,2`-bipyridine (bpy)

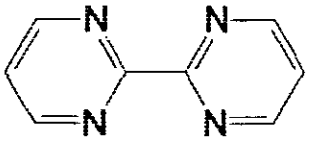

2,2`-bipyrimidine (bpym)

Fig. 1.12: Structures, abbreviation and names of bridging ligands

The ligands used in this study are given in Figure 1.2

In a long term we would like to explore the possibility of usage of these complexes in solar energy harvesting technology and to study their ability to act as efficient conductors.

CHAPTER 2

EXPERIMENTAL

2.1 Materials

All synthesis was performed under dry nitrogen. All photochemical reactions were performed in a specifically designed quartz reaction vessel fitted with a reflux condenser and a gas bubbler. A stirrer was also incorporated to ensure that the temperature was even throughout the solution. A 125 W-mercury arc broadband UV immersion lamp was used as the irradiation source and reflectors placed around the reaction vessel to maximize efficiency. A 313 nm, 150 W medium pressure lamp was also used. Tetrahydrofuran (THF) used in synthesis were of analytical grade and was further dried by molecular sieves. Hexane was dried on molecular sieves before used. Nitrogen gas used for purging was obtained from African Oxygen Limited (AFROX). Tungsten hexacarbonyl was obtained from Aldrich. The ligands are 2,2-biquinoline (Lancaster), 2,3-bis (2-pyridyl)pyrazine (Aldrich), 2,2-bipyrimidine (Lancaster), and 2,2-bipyridine (Merck). All reagents were used as supplied. The complexes

were purified by column chromatography (silica gel) which had been obtained from BDH laboratory supplies.

2.2. Instrumentation

2.2.1. Microanalysis

Microanalysis was carried out by University of North London (Faculty of Science, computing and Engineering) laboratory in UK and all the preparations were performed at the Chemistry Department at Imperial college, United Kingdom and University of Zululand, South Africa. Table **3.2** shows the results.

2.2.2 NMR spectroscopy

^{1}H NMR spectra were recorded using a JNM-EX270FT NMR spectrometer and data reported using the chemical shift scale units of ppm relative to $SiMe_4$ (TMS).

2.2.3. Mass Spectrometry

Fast atom bombardment (FAB) mass spectra were recorded on KRATOS MS-50 spectrometer, with either 3-nitrobenzyl alcohol or thioglycerol as a matrix and CsI as a calibrant.

2.2.4. IR spectroscopy

Infrared spectroscopy was carried out using Perkin-Elmer Paragon 1000 FT-IR solution cells (path length 0.5 mm) and a solid state spectrum in compressed KBr pellets. All values quoted are in wavenumbers (cm^{-1}). This technique was used to monitor the reaction and identification of products.

2.2.5. Electronic (UV-Visible) spectroscopy

Electronic (UV-visible) spectra were measured in dichloromethane and tetrahydrofuran on lambda 20 (UV/Vis spectrometer). This technique was used to monitor the reaction and identification of products.

2.2.6 Cyclic voltammetry

This technique has been used to evaluate the effect of ligand on the oxidation/reduction potential of the central metal ion in complexes and multinuclear clusters. It enables the electrode potential to be scanned rapidly in search of redox couples. This type of information plays an integral part in many of the approaches directed towards solar energy conversion. Cyclic voltammetric studies were carried out on Princeton Applied Potentiostatic/Galvanostat. Model 283.

2.2.7 Photoluminiscence

Emission spectra were carried out using Varian Cary 400 spectrophotometer. Photoluminiscence spectra were measured in dichloromethane. This technique is used to study emission on complexes. After complexes have absorbed radiant energy and excited to a higher electronic state, they must lose their excess energy in order to return to the ground electronic state.

2.3. Preparation of complexes

2.3.1 Synthesis of complexes of 2,3-bis(2-pyridyl)pyrazine.

$W(CO)_6$, (0.3 g, 0.768 mmol), was dissolved in 180 mL of dry THF and photolysed under an inert atmosphere of dry nitrogen gas for 8 minutes at ambient temperature using 125 W UV lamp.

The resulting yellow solution of tungsten pentacarbonyl tetrahydrofuran, $[W(CO)_5THF]$, was transferred into the 10 mL THF solution of 2,3-bis(2-pyridyl) pyrazine,(0.089 g, 0.383 mmol). The reaction mixture was stirred overnight at room temperature, in the dark and under nitrogen. The resulting dark purple solution was rotary evaporated to dryness at 40-50 °C yielding a dark purple paste. The product {$[W(CO)_4BPP]$, BPPM} was dissolved in dichloromethane and layered with hexane for crystallisation. An alternative route involved irradiation of a solution of 2,3-bis(2-pyridyl)pyrazine and finely ground tungsten hexacarbonyl in dry N_2-purged hexane, dichloromethane, or tetrahydrofuran (THF) at λ= 313 nm using a 200 W medium pressure tungsten lamp. After 8-10 minutes reaction time a dark purple solution was obtained as expected. Column chromatography was carried out on silica gel. Elution was done with pure dichloromethane. The products were recovered by rotary

evaporation. Thin layer chromatography, melting point and microanalysis was used to establish purity.

Anal. Calcd [$W(CO)_4BPP$], $C_{18}H_{10}N_4O_4W$} : 40.80%C, 1.89%H, 10.56%N. Found : 40.83%C, 1.80%H, 10.46%N.

Anal. Calcd [$\{W(CO)_4\}_2BPP$], $C_{22}H_{10}N_4O_8W_2$) : 31.96%C, 1.22%H, 6.78%N. Found : 32.56%C, 1.23%H, 6.98%N.

^1H NMR($C_{18}H_{10}N_4O_4W$) : δ = 8.80(d), 7.21(d), 8.10(d), 9.22(d), 7.60(t), 7.24(t), 8.60(t), 7.63(t), 8.60(d), 9.32(d).

^1H NMR($C_{22}H_{10}N_4O_8W_2$) : δ = 8.95(s), 8.45(d), 7.68(t), 7.96(t), 9.15(d)

Mass spectrometery($C_{18}H_{10}N_4O_4W$) : *m/z* 530[M^+], *m/z* 502[M^+-CO], and *m/z* 418[M^+-4CO].

Mass spectrometery($C_{22}H_{10}N_4O_8W_2$) : *m/z* 826[M^+], *m/z* [M^+-2CO]

IR(KBr), $\nu_{(CO)}$, 1816, 1837, 1879,1903, 2000 cm^{-1} for $C_{18}H_{10}N_4O_4W$

IR(KBr), $\nu_{(CO)}$, 1815, 1878, 1903, 2006 cm^{-1} for $C_{22}H_{10}N_4O_8W_2$

UV-Vis (CH_2Cl_2) for $C_{18}H_{10}N_4O_4W$: λ_{Max} = 520 nm

UV-Vis (CH_2Cl_2) for $C_{22}H_{10}N_4O_8W_2$: λ_{Max} =560, 617 nm

Photolumiscence : λ_{em} = 631, 439 for [$W(CO)_4BPP$]

: λ_{em} = 467 for [$(W(CO)_4)_2BPP$]

2.3.2. Synthesis of complexes of 2,2`-biquinoline

Photolysis of $W(CO)_6$ was carried out as described above. The resulting yellow solution was transferred in the dark to a THF (10 mL) solution of 2,2`-biquinoline (0.0984 g, 0.384 mmol). The resulting reaction mixture was stirred overnight at room temperature, in the dark and under inert atmosphere of nitrogen. The resulting dark blue solution was rotary evaporated to dryness at 40-50 °C yielding a dark blue oily material. This crude product was proven to contain a mixture of unreacted 2,2`-biquinoline ligand, as well as the desired mononuclear complex, {[$W(CO)_4$BQN], $C_{22}H_{12}N_2O_4W$}, and dinuclear complex, $C_{28}H_{12}N_2O_{10}W_2$, which was separated by thin layer chromatography. Direct photolysis of the ligand 2,2`-biquinoline and $W(CO)_6$ was also attempted due to the high efficiency and specificity possible *via* this route, this method was adopted. Column chromatography was carried out on silica. The crude product was dissolved in THF and dispersed on silica. Elution was first done with 80/20 CH_2Cl_2/hexane followed by 50/50 THF/CH_2Cl_2 and lastly 50/50 CH_3OH/ CH_2Cl_2. The product was recovered by rotary evaporation and further purified by washing with hexane. Thin layer chromatography, microanalysis and melting points were also done.

Crystallisation for [$W(CO)_4$BQN] was done using dichloromethane and hexane layering. The binuclear [{$W(CO)_5$}$_2$BQN] decompose on the column, so no analysis has been done.

Anal. Calcd ($C_{22}H_{12}N_2O_4W$): 47.8 %C, 5.1 %H, 2.17 %N. Found: 47.68 %C, 4.92 %H, 2.09 %N.

Anal. Calcd ($C_{12}H_6N_4O_4W$): 31.7 %C, 1.3 %H, 12.3 %N. Found: 31.6 %C, 1.2 %H, 12.4 %N.

^1H NMR ($C_{22}H_{12}N_2O_4W$): δ = 8.24(d), 7.59(t), 7.75(t), 8.86(d), 8.34(d), and 7.89(d)

IR (KBr): 1811, 1868, 1896, 2000 cm^{-1}

UV-Vis(CH_2Cl_2), $C_{22}H_{12}N_2O_4W$: λ_{Max} = 576 nm

Photolumiscence: λ_{em} = 462 nm

2.3.3 Synthesis of 2,2`-bipyrimidine complexes

2,2-Bipyrimidine (0.0607 g, 0.384 mmol) was reacted with finely grounded tungsten hexacarbonyl (0.3 g, 2.0 mmol) in dry N_2-purged dichloromethane (150 ml) by UV-irradiation at λ = 313 nm, 150 W medium pressure lamp. After 15-20 minutes a brown solution was obtained. The solvent was subsequently removed in *vacuo* and the crude products separated by thin layer chromatography. The solution was taken to dryness by rotary evaporation. The residue, the mononuclear, binuclear complexes and some

starting materials were separated by column chromatography on silica using pure tetrahydrofuran as an eluent.

Anal. Calcd ($C_{12}H_6N_4O_4W$): 31.7 %C, 1.3 %H, 12.3 %N. Found: 31.6 %C, 1.2 %H, 12.4 %N.

Mass Spectrometry: *m/z* 454 [M^+], 426 [M^+-CO] and 398 (M^+ -2CO)

IR (KBr), $\nu_{(co)}$, 1824, 1864, 1904, 2004 cm^{-1} for $C_{12}H_6N_4O_4W$

IR (KBr), $\nu_{(co)}$, 1826, 1889, 1919, 2005 cm^{-1} for $C_{16}H_6N_4O_8W_2$

UV-Visible (CH_2Cl_2), $C_{12}H_6N_4O_4W$: $\lambda_{\pi\rightarrow\pi^*}$ = 300 nm, 379 nm and λ_{MLCT} = 543 nm

UV-Visible (CH_2Cl_2), $C_{16}H_6N_4O_8W_2$: λ_{MLCT} = 457 nm, 725, 813 nm

Photoluminiscence: λ_{em} = 653, 494, 327 for [$W(CO)_4$BPYM]

λ_{em} = 505 for [{$W(CO)_4$}$_2$BPYM]

2.3.4 Synthesis of Tetracarbonyl-2,2-bipyridine tungsten

A similar procedure to the 2,2′-bipyrimidine was used to prepare [W(CO)$_4$bpy] i.e. 2,2`-bipyridine (0.0599 g, 0.383 mmol). The plum coloured suspension changed to a dark red solution after 15-20 minutes. The solvent was removed in *vacuo* to yield the crude mononuclear complex. The product was separated by column chromatography on silica.

Anal. Calcd ($C_{14}H_8N_2O_4W$): 37.2 %C, 1.8 %H, 6.2 %N. Found:

37.1 %C, 1.7 %H, 6.2 %N.

Mass Spectrometry: *m/z* 452 [M^+], 424 [M^+-CO] and 396 (M^+ -2CO)

IR (KBr): 1811, 1865, 1909, 2003

UV-vis(CH_2Cl_2), $C_{14}H_8N_2O_4W$: λ_{Max} = 350, 485 nm

Photoluminescence: λ_{em} = 597, 497, 410 nm

Chapter 3- *Results and Discussions*

3.1 Complexes of 2,3-bis(2-pyridy)pyrazine

The compounds are typically stable as solids, though they are somewhat light and air sensitive. At room temperature, solutions of the complexes are moderately stable, with the chromium complexes exhibiting the vast instability and could not be investigated further. Decomposition was, however, generally slow for the other compounds and was only troublesome in polar media.

Irradiation of $[M(CO)_6]$ in rigid media at low temperature yields spectral changes consistent with the loss of CO to generate C_{4V} $[(OC)_5M(pyz)M'(CO)_5]$ species. The IR spectra supported assignment of the primary photoproduct as C_{4V}, $[M(CO)_5THF]$. Overnight stirring of THF adducts and the selected ligand results in desired products.

This species reacts easily with the ligands at room temperature by exchanging the THF ligands. Confirmation with literature data supports the intermediate product[40].

$$[M(CO)_6] + THF \xrightarrow{h\nu,\ 125W} [M(CO)_5THF]$$

$$[M(CO)_5THF] \xrightarrow{L} [M(CO)_4L] + THF$$

THF is weakly bound, and a pure $[M(CO)_5L]$ or $[M(CO)_4L]$, bidentate ligand (L), species is obtained by addition of ligand to the solution of, $[M(CO)_5THF]$, as in the equations above. This method has the disadvantage that it requires many reactions to gradually build up the structure and so is a slow process, the yield is reduced at each step.

An alternative route was found to be the more appropriate and convenient. It is also less time consumption. Direct photolysis of CH_2Cl_2 solution of $[M(CO)_6]$ with the ligand took only 8 minutes for the reaction to be complete. Irradiation time stopped at this point followed by solvent removal in *vacuo*. Evidence of colour change in the reaction generally from yellow to dark purple within 8-10 minutes was a good indication that the reaction was reasonably fast. Irradiation of THF with the ligand was also attempted. The method was abandoned due to the fact that the THF ligand competes with the selected ligand giving unexpected products, which makes isolation difficult. However, whilst some of the desired product was formed, some side reaction also seemed to take place. Hence mixture of the desired complex and THF substituted products are formed. It might be interesting to carry out reactions in different solvents. This method is ideal for the ligand that is photoactive.

$$M(CO)_6 + L \xrightarrow[CH_2Cl_2]{hv,\ 313nm} M(CO)_4L + 2CO \ ,$$

for bidentate ligand(L)

It was previously recognized from the outlet that photolysis of $[M(CO)_5L]$ could result in the loss of another CO molecule or loss of L.

Elution with pure dichloromethane gives the products in the order $\{[(W(CO)_4)_2BPP], BPPD\}$ and then $\{[W(CO)_4BPP], BPPM\}$. Methanol elutes the remaining BPP{2,3-bis(2-pyridyl)pyrazine} ligand.

Alternatively, washing the crude product with cold hexane could effect the separation of $\{[W(CO)_4BPP], BPPM\}$ and $\{[(W(CO)_4)_2BPP], BPPD\}$. Solubility differences of each of the compounds BPPD, BPPM and the starting materials mean that work up of the mixture is made easier. The starting materials and BPPD were found to be soluble in hexane, but BPPM is soluble only in THF. Hence washing the solid product mixture with hexane and then with THF leads to an effective separation of the BPPM. It should be noted that more of the dimer, $[(W(CO)_4)_2BPP]$ can be obtained by increasing the ratio of tungsten hexacarbonyl. This compound has proven to be unstable in solution, so it must be stored as solid (storing under nitrogen greatly increased their long-term stability). If they are to be

studied in solution, this must be done as rapidly and in the absence of air where possible. The tungsten complexes were chosen over the chromium or molybdenum materials because of their high thermal and atmospheric stability. Scheme 3.1 that illustrate the synthesis of the complexes.

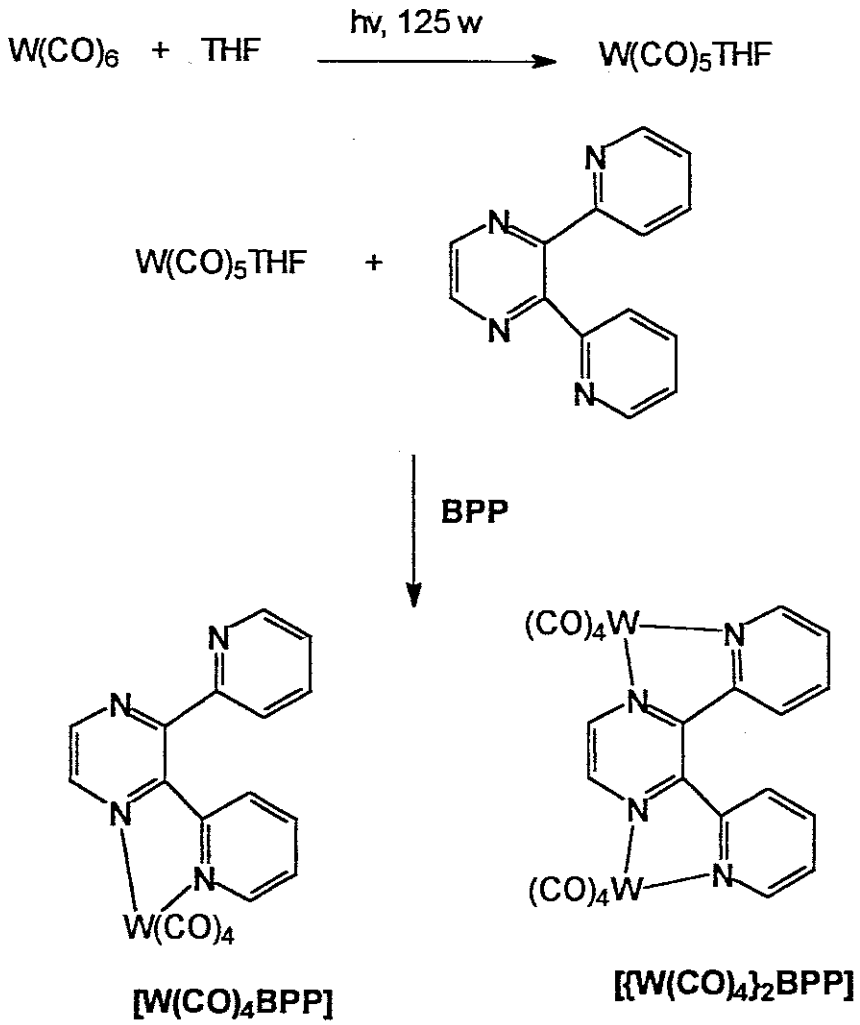

Scheme 3.1

3.1.1 Microanalysis, thin layer chromatography and melting point

Sharp melting point, single spot on thin layer chromatography and elemental analysis (C, H, N) confirm the purity of the complexes as depicted in Table 3.1. Dimers have lower melting point than monomers due to the fact that the metal to ligand bond strength is weaker as compared to monomers.

Table 3.1. Microanalysis and melting point data

Complex	Colour	Melting point	Microanalysis(calculated)		
			%C	%H	%N
$[W(CO)_4BPP]$	Dark purple	194-5	40.8 (40.8)	1.8 (1.9)	10.5 (10.6)
$[\{W(CO)_4\}_2BPP]$	Dark green	165	32.56 (31.96)	1.23 (1.22)	7.0 (6.8)
$[W(CO)_4BQN]$	Dark blue	200	47.7 (47.8)	4.9 (5.1)	2.1 (2.2)
$[W(CO)_4BPYM]$	Dark brown	180	31.6 (31.7)	1.2 (1.3)	12.4 (12.3)
$[\{W(CO)_4\}_2BPYM]$	Dark green	163			
$[W(CO)_4BPY]$	Dark red	210	37.1 (37.2)	1.7 (1.8)	6.3 (6.2)

3.1.2 Mass spectroscopy

A molecular ion peak M^+ at *m/z* 530 for the mononuclear species,$[C_{18}H_{10}N_4O_4W]$, was observed. Fragment ion appears at *m/z* 502 due to loss of carbon monoxide molecule. A strong fragment ion also appears at *m/z* 418 due to the loss of four carbon monoxide molecules. The mass spectrum for, $[C_{18}H_{10}N_4O_4W]$ is shown in Figure 3.1.

Fast atom bombardment (FAB) mass spectrometry of the dimeric complex, $[C_{22}H_{10}N_4O_8W_2]$ reveals a molecular ion peak M^+ at M/Z 826. Fragment ion appears at *m/z* 770 due to loss of two carbon monoxide molecules. The mass spectrum of $[C_{22}H_{10}N_4O_8W_2]$ is represented in Figure 3.2. This fragmentation patterns are in good agreement with the structure of the complexes and mass spectra obtained and hence confirms the products.

This mass spectrometry agrees with the nitrogen rule, which state that: "If a compound contains an even number of nitrogen atoms, its molecular ion will be at an even mass number."

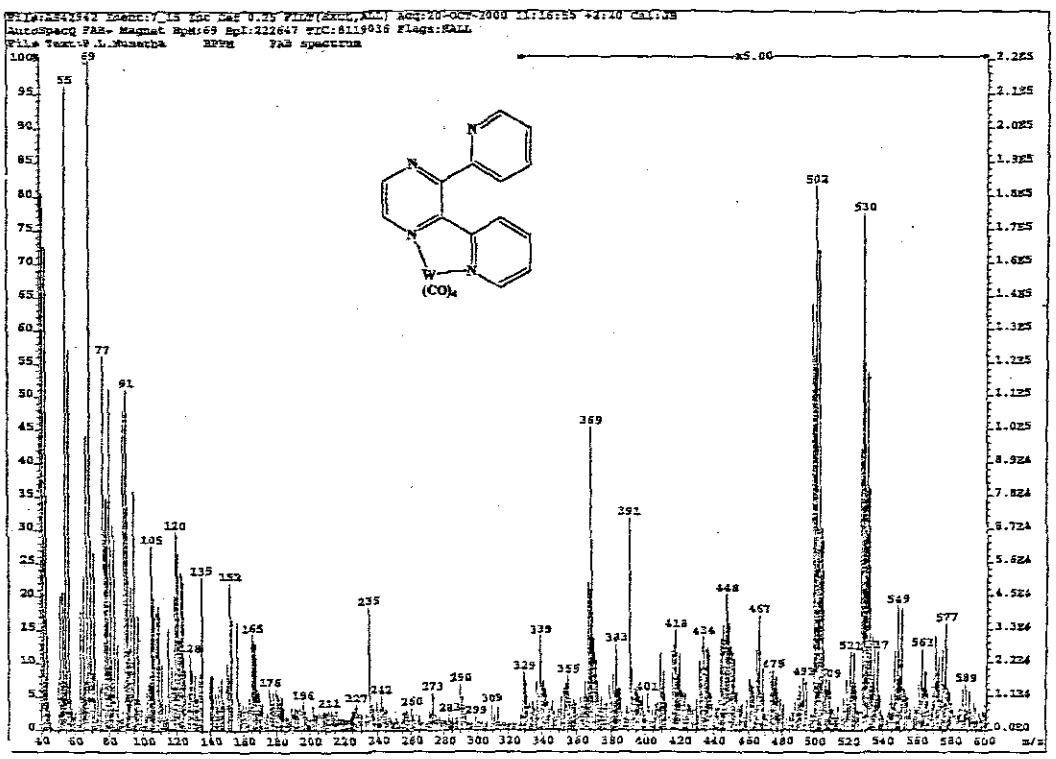

Figure 3.1_ Mass spectrometry for [W(CO)$_4$bpp]

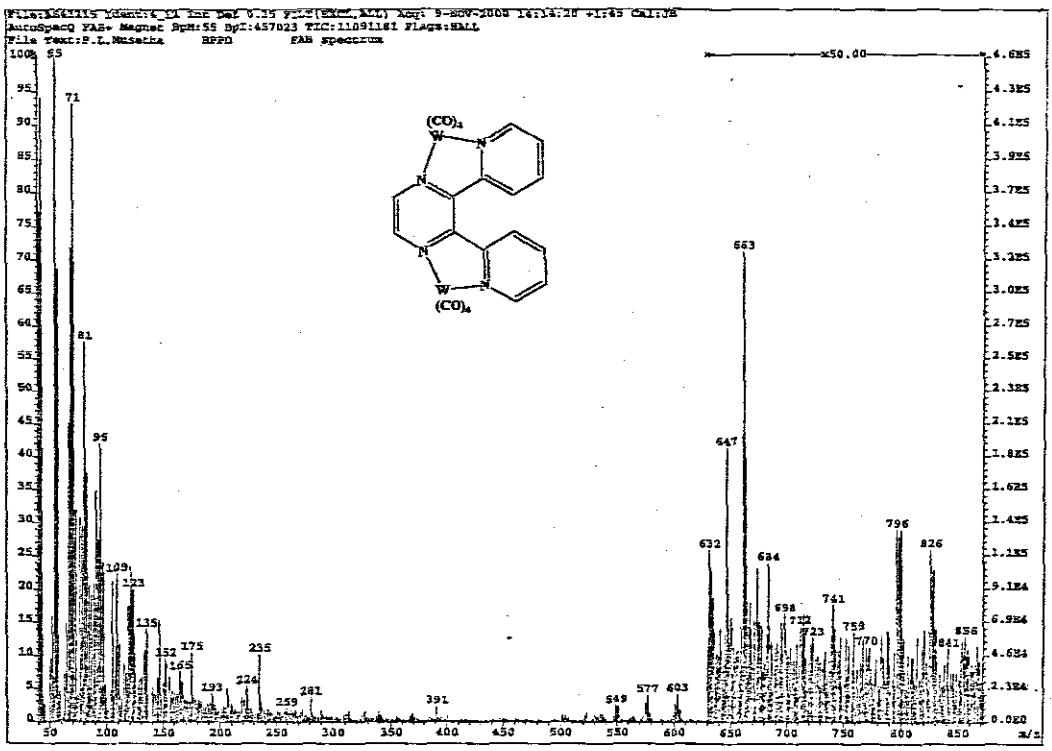

Figure 3.2_Mass spectrometry for [{W(CO)$_4$}$_2$bpp]

3.1.3 ^{1}H NMR spectroscopy

The ^{1}HNMR spectrum of the mononuclear complex, [$C_{18}H_{10}N_4O_4W$] and binuclear complex, [$C_{22}H_{10}N_4O_8W_2$] are illustrated in Figures 3.4 and 3.5. The ^{1}H NMR for [$C_{22}H_{10}N_4O_8W_2$] in chloroform-d and acetone-d_6 proved

unsuccessful so d_6-DMSO was then used and good signals were observed. A disadvantage in using DMSO is that product recovery in most cases proves impossible. Ten signals for the unsymmetrical monomeric complex were observed as expected and for the dimer only five signals were obtained. The signals at 7.20 ppm (H_7) and 8.10ppm (H_{10}) were due to the protons neighbouring nitrogen bound to the metal. The ^1H NMR spectrum of the binuclear compound showed two sets of doublets at 9.14 ppm for protons nearest to nitrogen bonded to tungsten and 8.47 ppm for the protons close to nitrogen farther away from the metal. In the binuclear complex, the symmetrical equivalence of the dimer H_3 and H_{10} share the same smaller Coupling, therefore the two rings is restored, so the protons appear in pairs as expected. H_1 (8.80) and H_2 (9.31) shares the same coupling because the two protons are near to nitrogen atoms, so they are expected to absorb at a

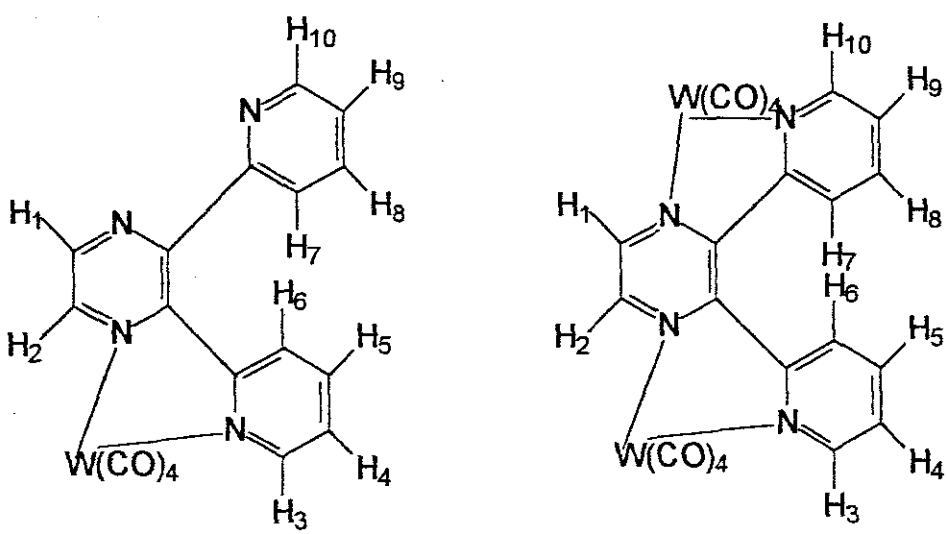

Figure 3.3_Structure of [W(CO)$_4$BPP] and [{W(CO)$_4$}$_2$BPP]

lower field.

A single peak is observed at 8.95ppm for protons H_1 and H_2 since they occupy identical environment with the same shielding. These protons are therefore chemically equivalent. The protons nearest to the electronegative atoms, i.e. oxygen and nitrogen, have a lower chemical shift due to the increase of deshielding of the nucleus. $[C_{18}H_{10}N_4O_4W]$ and $[C_{22}H_{10}N_4O_8W_2]$ retain same symmetry properties and it is this fact that governs the closeness in the ^1H NMR spectra, both approximate C_{2v} symmetry. ^1H NMR spectra indicate the distinguishable proton resonances for each complex are consistent with this formulation. This appears to confirm the proposed structures of the complexes. Table 3.2 shows the results.

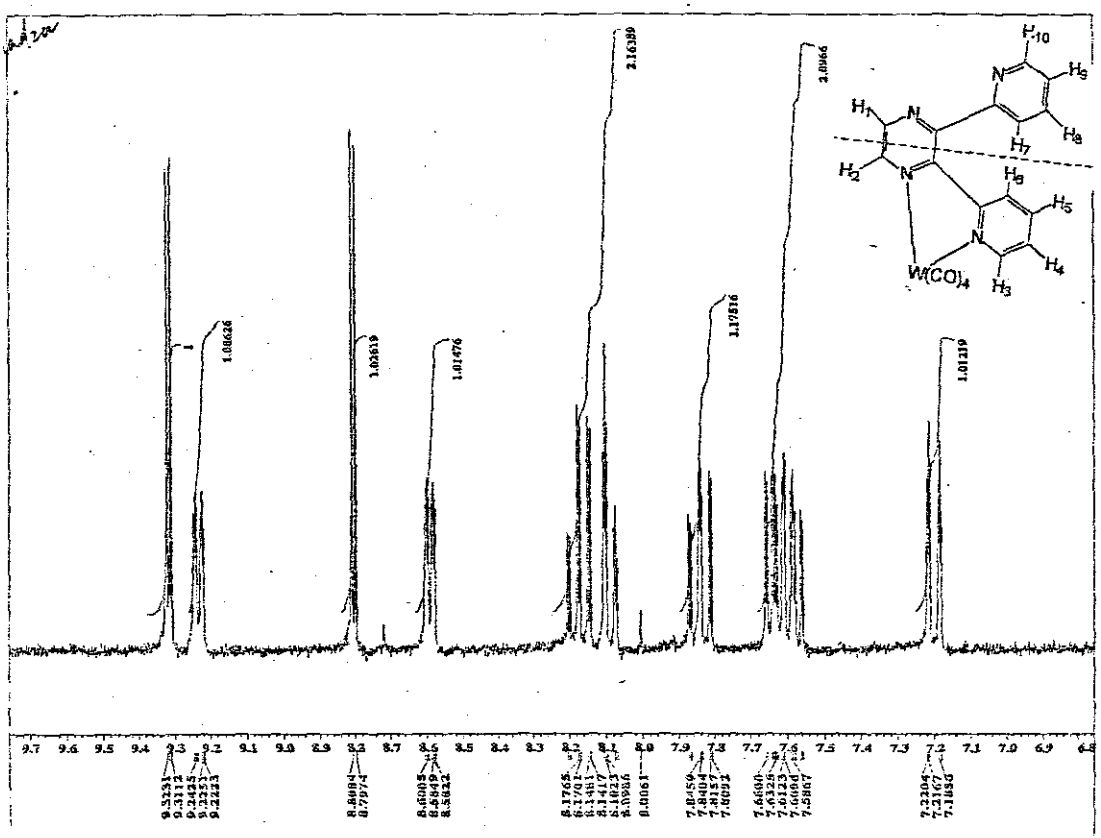

Figure 3.4_ ^{1}HNMR for W(CO)$_4$bpp

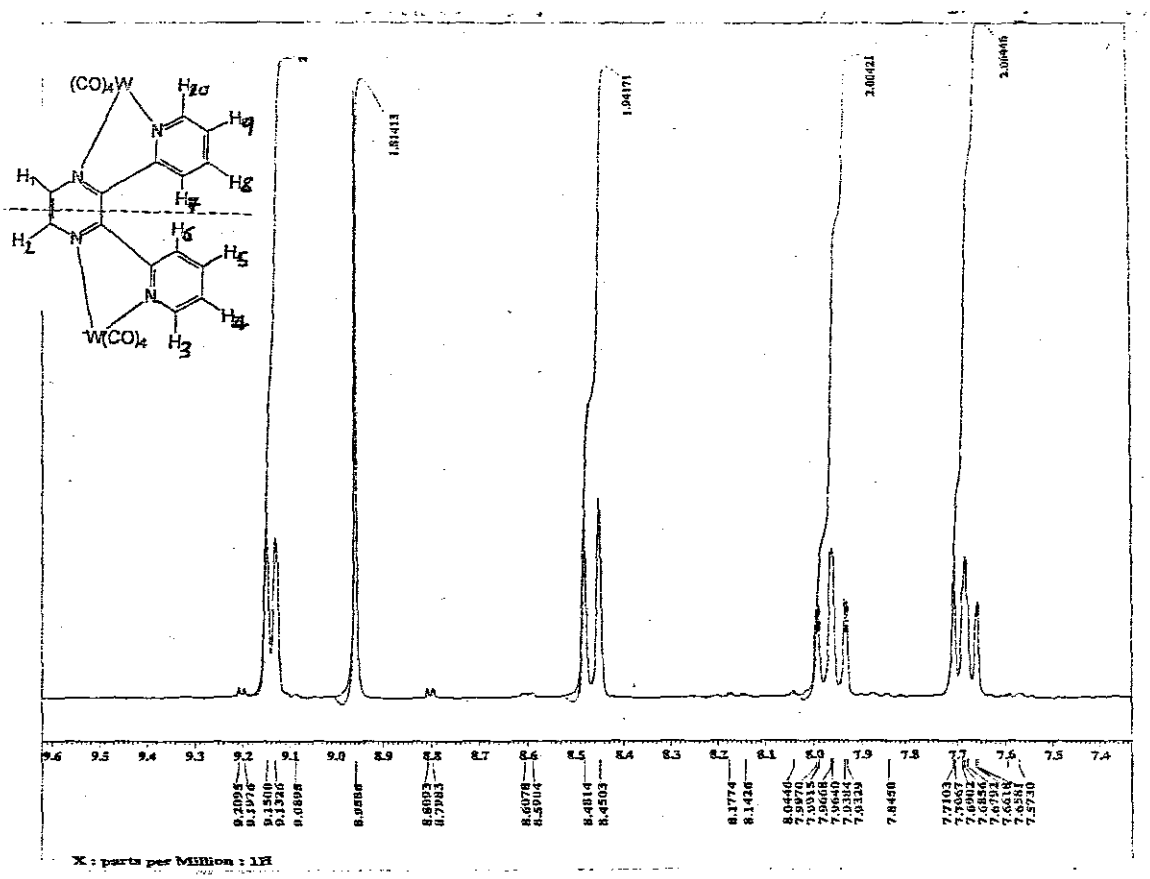

Figure 3.5_ ^{1}HNMR for [{W(CO)$_4$}$_2$bpp]

Table 3.2. ^{1}HNMR for $[W(CO)_4BQN]$, $[W(CO)_4BPP]$, and $[\{W(CO)_4\}_2]$

$[W(CO)_4BQN]$	Proton no.	$[W(CO)_4BPP]$	$[\{W(CO)_4\}_2]$
8.22(d)	H_1	8.80(d)	8.96(s)
7.57(t)	H_2	9.31(d)	
7.75(t)	H_3	9.23(d)	9.14(d)
	H_{10}	8.10(d)	
7.88(d)	H_4	7.63(t)	7.69(t)
	H_9	8.17(t)	
8.84(d)	H_5	7.84(t)	7.96(t)
	H_8	7.61(t)	
8.32(d)	H_6	8.59(d)	8.47(d)
	H_7	7.20(d)	

3.1.4. IR Spectroscopy

Infrared spectra were taken as KBr discs. IR first did Observation/monitoring of the progress of the reaction in the UV reactor and the identification of the products of the reaction with the ligand. The infrared spectrum for $[W(CO)_5THF]$ shows three peaks, a single sharp peak at 1930. The spectra obtained showed splitting of the parent metal hexarbonyl from singlet into a triplet. This suggests that only one of the carbonyl in the parent hexacarbonyl has been substituted and the product contains therefore a pentacarbonyl moiety.

The $[M(CO)_5THF]$ complex exhibit three moderate/strong bands, these are assigned to A_1^1 , E , and A_1^1 modes, in accordance with the local C_{4v} symmetry of the carbonyl ligands. Focussing on the carbonyl region, the 3 moderate/strong band maxima are assigned to A_1^1, E and A_1^2 modes and are characteristic of C_{4V} arrangement of the carbonyl ligand at the metal center[6,39,43].

The carbonyl frequencies are closely related to those previously reported indicating that the local symmetry of the $M(CO)_5$ is C_{4v}. The IR for $[W(CO)_5THF]$ is depicted in Figure 3.6.

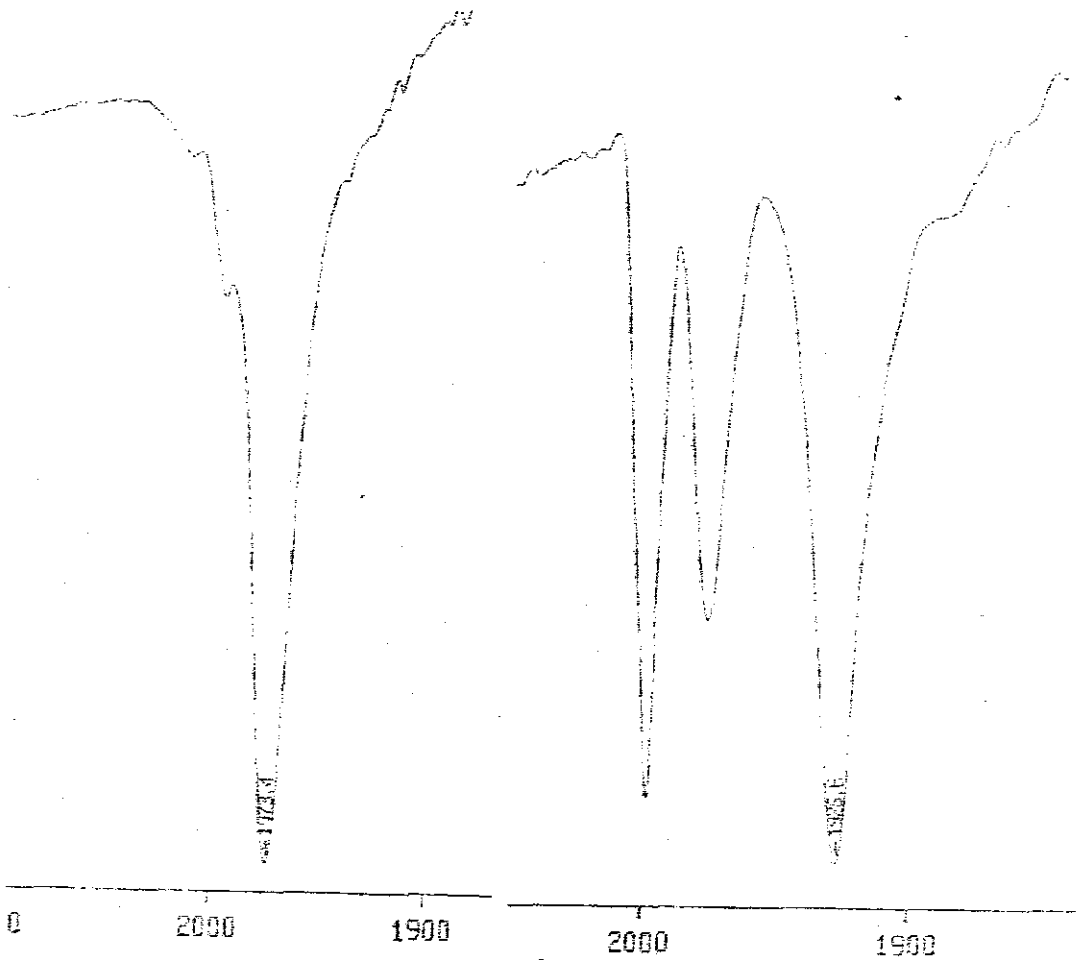

Figure 3.6_ IR for [$W(CO)_5THF$]

The IR spectra for the products showed that the carbonyl stretching peaks of the tungsten center adopts a C_{2v} symmetry and were consistent with *cis*-substituted tungsten tetracarbonyl complexes as only four υ_{CO} bands near 1900 cm^{-1} were observed. Main peak for tetracarbonyl appears at

1890 cm^{-1}. The CO stretching frequencies of the carbonyl complexes depend on the number of CO neighbours in the complex. An additional band at 1837 cm^{-1} is assigned to a small amount of $W(CO)_6$ formed upon decomposition. Infrared spectra are depicted in Figures 3.7 and 3.8 for both the mononulear, $[C_{18}H_{10}N_4O_4W]$ and the binuclear, $[C_{22}H_{10}N_4O_8W_2]$.

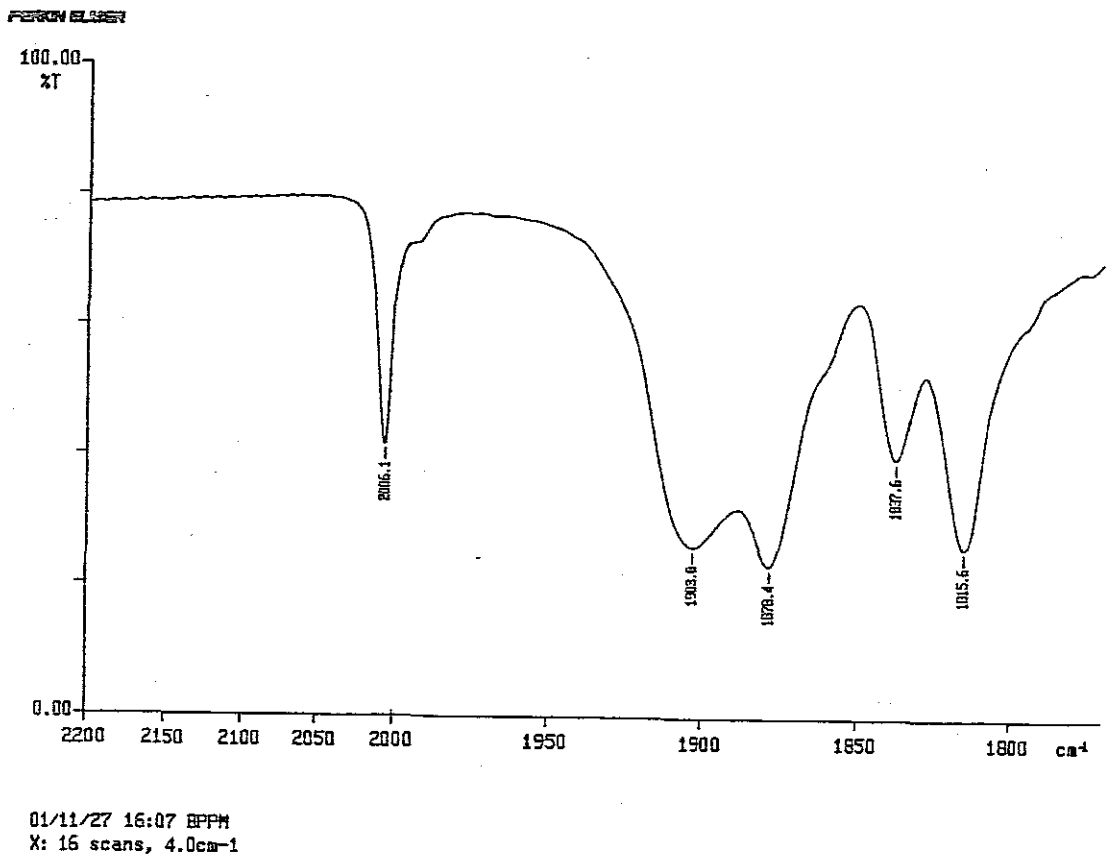

Figure 3.7_IR for $[W(CO)_4bpp]$

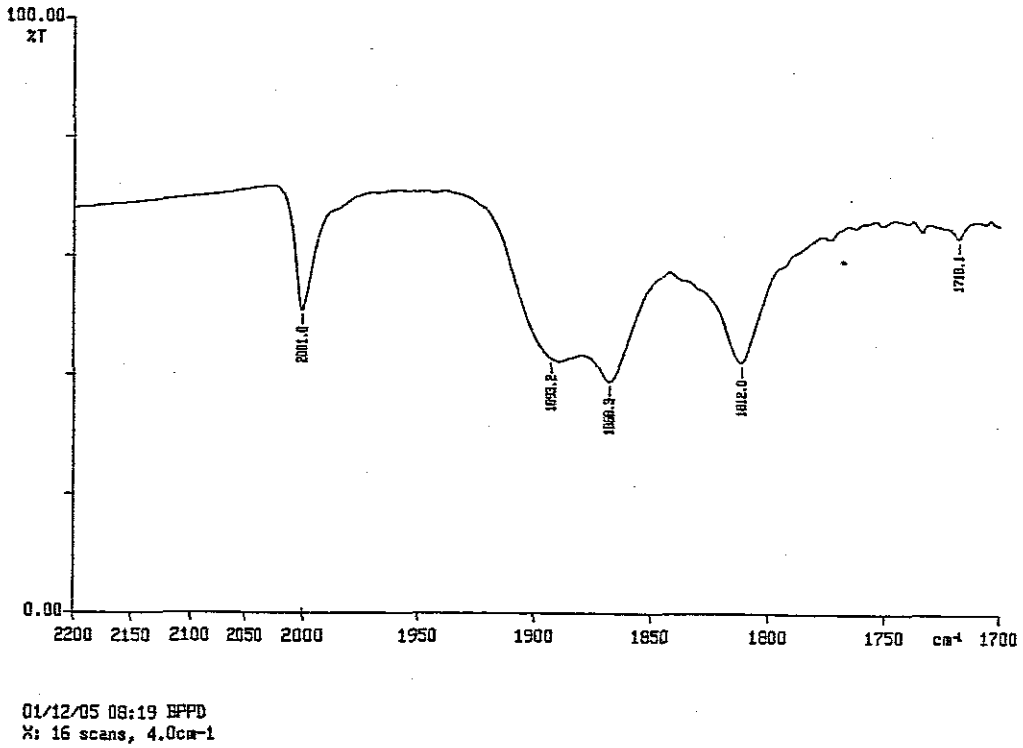

Figure 3.8_ IR for [{W(CO)$_4$}$_2$bpp]

Table 3.3. Vibrational stretching frequencies ν_{CO}[cm^{-1}] of bpp,bqn, bpym, and bpy complexes.

Complex	Tetracarbonyls			
	A_1(s)	B_1(vs)	A_1(sh)	B_2(s)
[W(CO)$_4$BPP]	2000	1903	1879	1816
[{W(CO)$_4$}$_2$BPP]	2006	1903	1878	1815
[W(CO)$_4$BQN]	2000	1896	1868	1811
[W(CO)$_4$BPYM]	2004	1904	1864	1824
[{W(CO)$_4$}$_2$BPYM]	2005	1919	1889	1826
[W(CO)$_4$BPY]	2003	1909	1865	1811

3.1.5 UV-Visible Spectroscopy

The $[C_{18}H_{10}N_4O_4W]$ and $[C_{22}H_{10}N_4O_8W_2]$ complexes exhibit C_{2v} symmetry. In the visible region, the absorption spectrum exhibits two bands that arise as results of MLCT absorptions. Comparison of the electronic spectrum of the mononuclear, $[C_{18}H_{10}N_4O_4W]$, with that of the binuclear $[C_{22}H_{10}N_4O_8W_2]$ reveals a shift of the $^1A_{1g} \rightarrow {}^1T_{1g}$ transition, in both, to longer wavelength and $^1A_{1g} \rightarrow {}^1T_{2g}$ to shorter wavelength. The absorption spectra of $[WCO)_4bpp]$ and $[\{W(CO)_4\}_2bpp]$ tungsten complexes of isomeric exhibit $[\{WCO)_4\}_2bpp]$ ligand centered bands in the UV region and broad metal-to-ligand (W→bpp) charge-transfer bands in the visible region. In C_{2v} complexes of unsaturated nitrogen donor ligands the MLCT and intraligand ($\pi \rightarrow \pi^*$) transitions are observable. When the BPP ligand is bound to only one metal centre, this transition occurs in the 550 nm. When BPP bridges more than one metal centre, the stabilization of the π^*-acceptor orbital on the BPP shift the MLCT transition to lower energy, at 560 and 617 nm. In other words the bands are red shifted in passing from the mononulear to the binuclear complexes. This spectrum is consistent with the assigned structure. The UV-visible spectra of the complexes are shown in Figures 3.9 and 3.10.

The results obtained are in good agreement with the literature[5,33,43,53,55].

Table 3.4 shows the results.

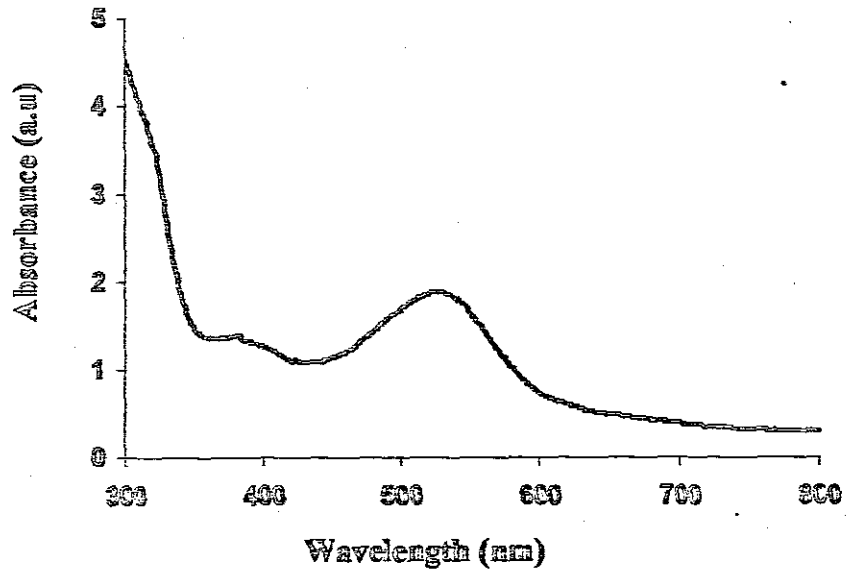

Figure 3.9 UV-visible for [W(CO)$_4$bpp]

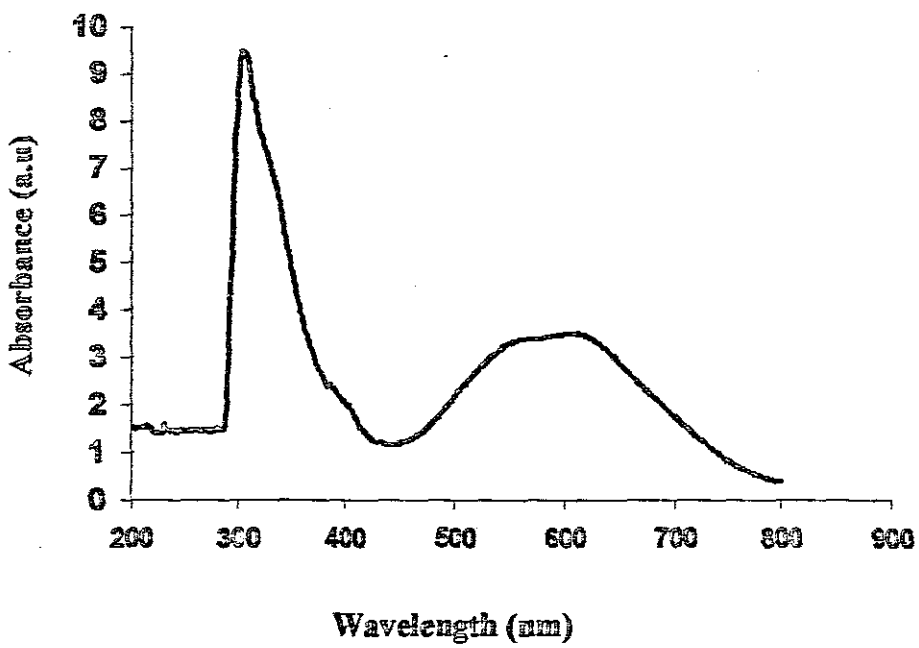

Figure 3.10_ UV-visible for [{W(CO)$_4$}$_2$bpp

Table 3.4 Electronic absorption and emission maxima for 2,3-bis(2-pyridyl)pyrazine, 2,2`-biquinoline, 2,2`-bipyrimidine, and 2,2`-bipyridine.

	$\lambda_{\pi\rightarrow\pi}$	λ_{MLCT}	λ_{em}
$[W(CO)_4BPP]$	300	520	439, 631
$[\{W(CO)_4\}_2BPP]$	300	560, 617	467
$[W(CO)_4BQN]$	390	576	462
$[W(CO)_4BPYM]$	350	485	410, 497, 597
$[\{W(CO)_4\}_2BPYM]$	300, 379	543	327, 494, 653
$[W(CO)_4BPY]$	457	725, 813	505

3.1.7 Photoluminiscence

This complex showed emission bands with maxima at about 439, and 631 nm in dichloromethane solution. These emissions are both assigned to metal-to ligand-charge transfer. For the binuclear complex $[\{W(CO)_4\}BPP]$, only one emission was observed at 467 nm which is assigned to MLCT. Figure 3.11 and 3.12 shows the results. Table 3.4 shows the results.

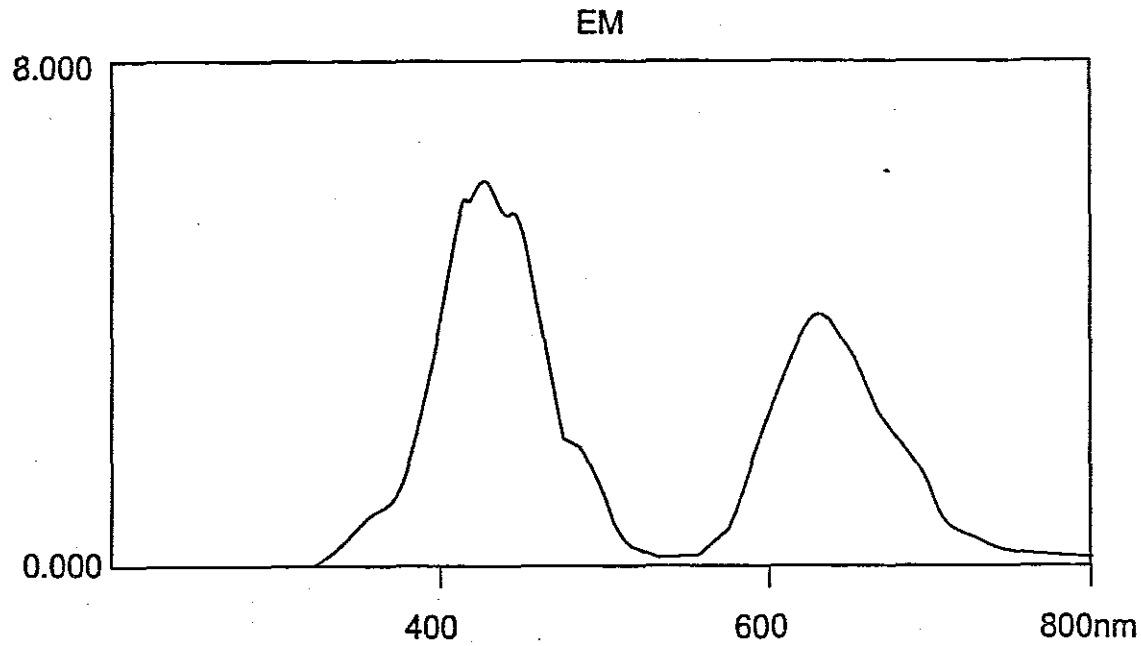

Figure 3.11_ Emission spectra for [W(CO)$_4$bpp]

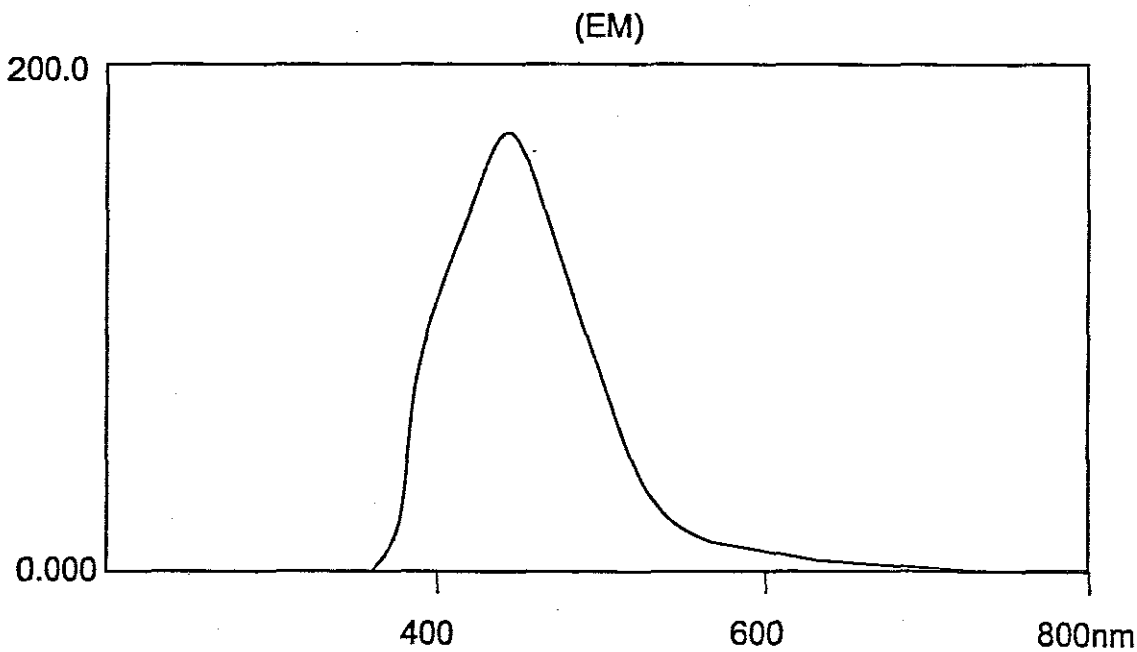

Figure 3.12 Emission spectra for [{WCO)$_4$}$_2$bpp}

3.1.8 Cyclic Voltammetry

An electrochemical measurement in the potential window from +1.2 to –3.0V vs SCE shows several waves. The mononuclear complex, $[W(CO)_4bpp]$ exhibits four oxidation wave at 0.728V, -0.445V, -2.001V and –0.296V. The reduction waves at 0.650V, -0.341V, and –1.935V. The redox potential exhibits reversible pairs of oxidation/reduction.

The binuclear complex, $[\{W(CO)_4\}_2bpp]$ exhibits three oxidation waves at 0.726V, -0.996, -2.21V and three reduction waves. Figure 3.13 and 3.14 shows the results.

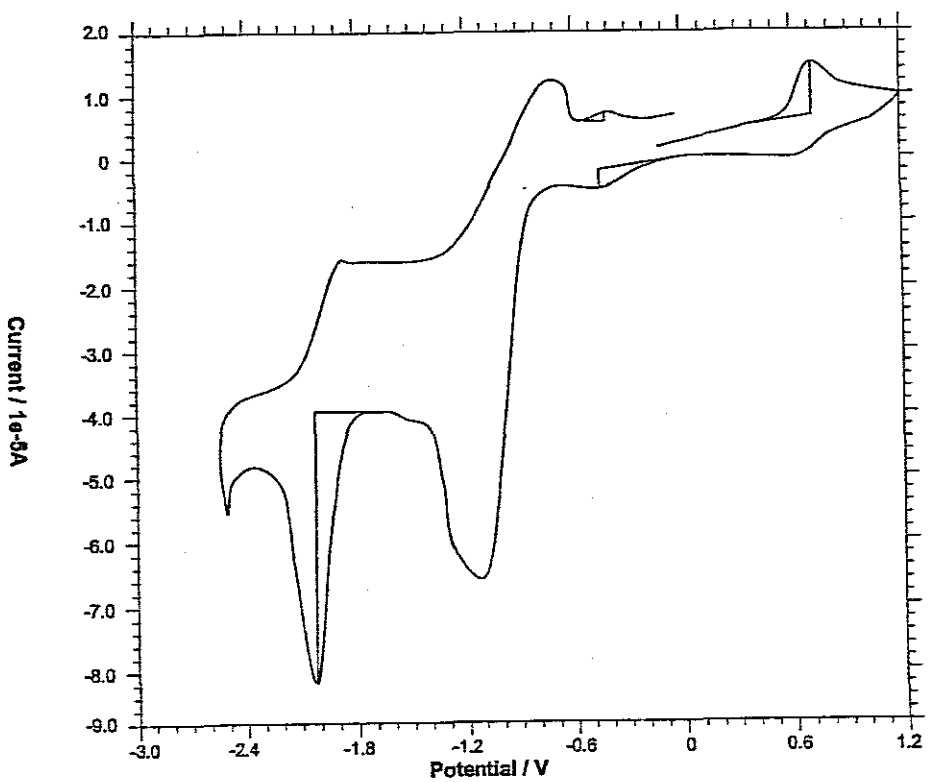

Figure 3.13_ Redox potential of $[W(CO)_4bpp$

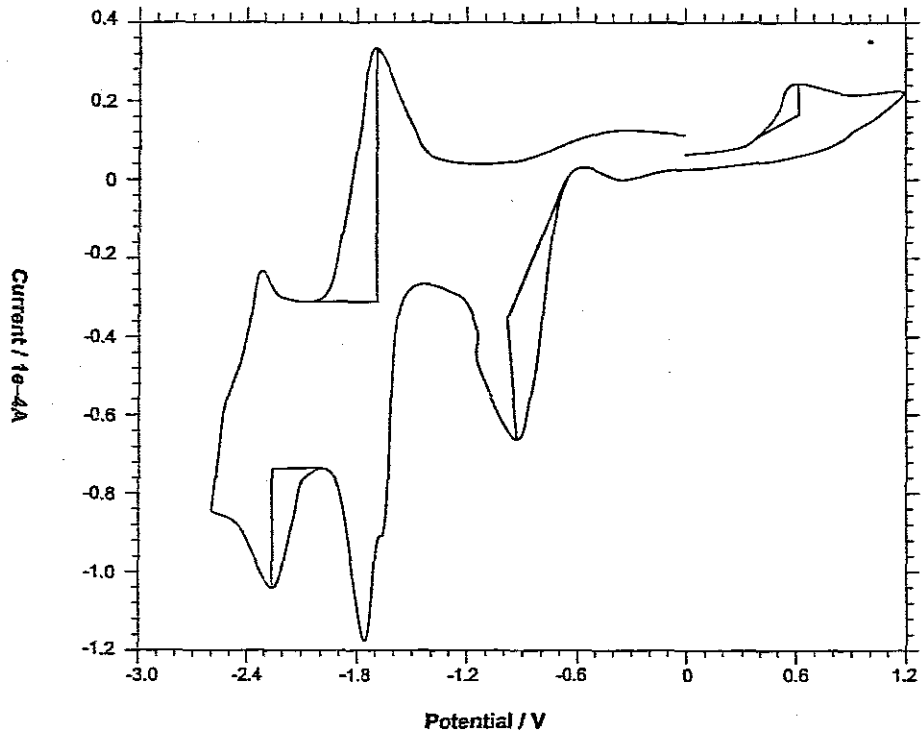

Figure 3.14_ Redox potential of [{W(CO)$_4$}$_2$bpp]

3.2 Complexes of BQN

3.2.1 Synthesis of complexes of BQN

Purification of the product mixture was enabled using column chromatography on silica gel. However, the dimeric product [{W(CO)$_5$}$_2$BQN] decomposed on the column. For this reason only the

mononuclear species, $[W(CO)_4BQN]$ could be obtained for 2,2'-biquinoline. Excess of tungsten hexacarbonyl was removed by vacuum sublimation. We have met with little success in attempts to synthesize the chromium complex of 2,2'-biquinoline. The stability of the complexes is dependent on the metal present, on whether they are stored in solution or as solid and in solvent in which they are dissolved e.g. complexes containing chromium are all air, moisture, and solvent sensitive at room temperature[38,48]. The greater the proportion of chromium, the greater the thermal decomposition. The reaction scheme is shown in Scheme 3.2 .

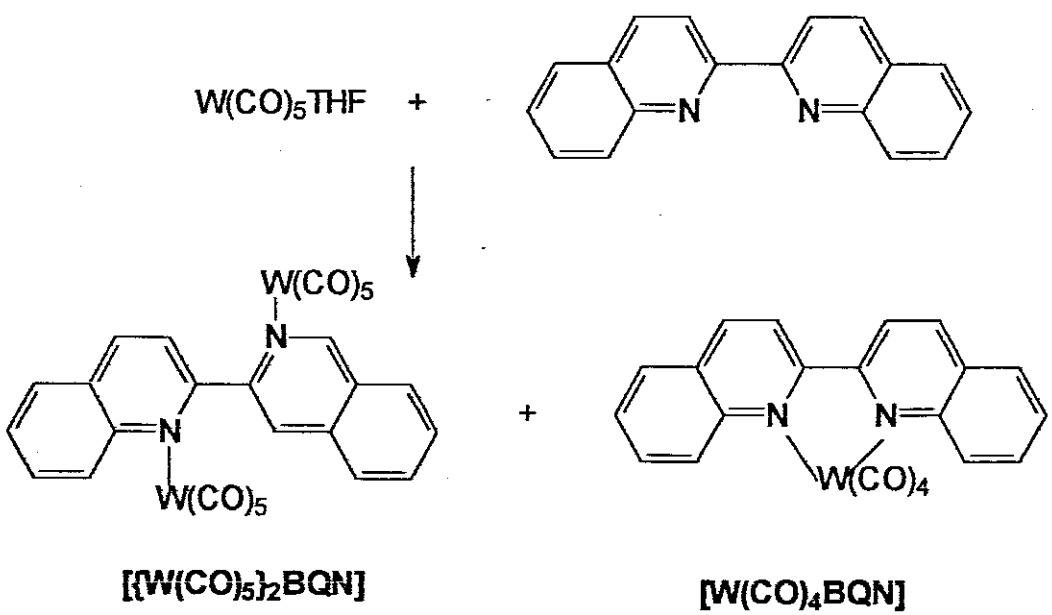

Scheme 3.2

Elution with 80/20 CH_2Cl_2 /hexane followed by 50/50 THF/ CH_2Cl_2 and then with 50/50 methanol/ CH_2Cl_2 leads to effective purification. Washing the product with cold hexane did further purification. The product was recovered by rotary evaporation.

3.2.2 Microanalysis, thin layer chromatography and melting point

Sharp melting point (200 °C), single spot on thin layer chromatography and elemental analysis confirm the purity of the complex as shown in Table 3.1.

3.2.3 Mass spectroscopy

Fast-atom bombardment (FAB) mass spectrometry of the monomeric complex [$C_{22}H_{12}N_2O_4W$] reveals a molecular ion peak M^+ at 550. Fragment ion appears at *m/z* 522 due to the loss of carbon monoxide. By convention in mass spectrometry, molecular ion species usually gives several isotopic peaks. The isotopic pattern of the single peaks, reflects the occurrence of the tungsten isotopes [180(0.13%); 182(26.3%); 183(14.3%); 184(30.6%); and 186(28.6%)]. This enables the tungsten containing fragments to be very easily identified. Figure 3.15 shows the results.

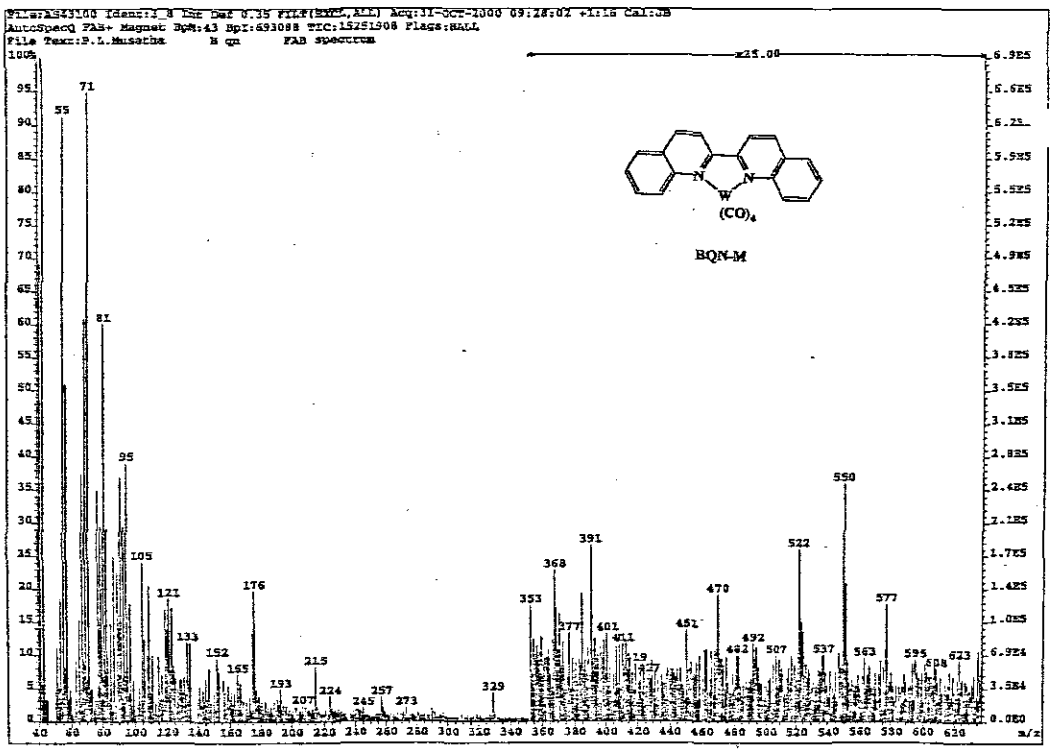

Figure 3.15_ Mass spectra for $[W(CO)_4bqn]$

3.2.4 ^{1}H NMR spectroscopy

The ^{1}H NMR spectra of $[W(CO)_4BQN]$ is shown in Figure 3.17. The ^{1}H NMR data is depicted in Table 3.2. Chloroform-d was used showing good signals as expected. Unidentified impurities at 9.75 ppm and 8.05 ppm

were observed. The ^{1}H NMR of the complex showed the presence of the six types of protons. Sharper doublets at 8.84 and 8.32 due to H_5 and H_6 because they are isolated from other protons/not affected by coupling. Triplets at 7.57 ppm and 7.75 ppm are due to H_2 and H_3. Two triplets at 7.59(t) and 7.75(t) were observed. The bond length and electronegative atoms was noted as the influence of deshielding of the nucleus.

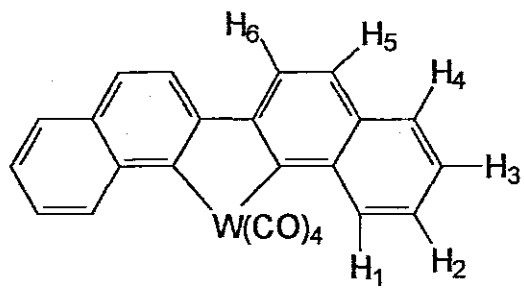

Figure 3.16 Structure of $W(CO)_4$BQN with labeled protons

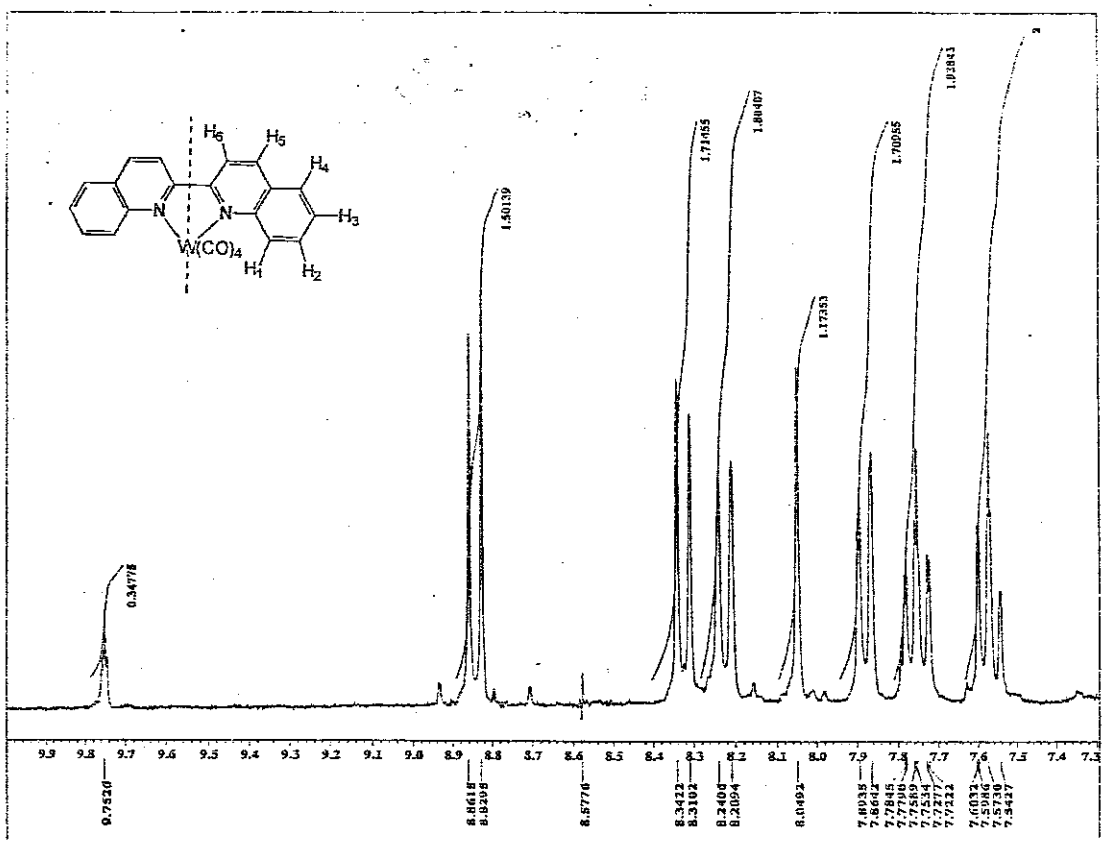

Figure 3.17_ ^{1}HNMR for [W(CO)$_4$bqn]

3.2.5 Infrared spectroscopy

The IR spectrum was taken as KBr disk. The spectra of this mononuclear complex, $[C_{22}H_{12}N_2O_4W]$ shows four bands in the 1800-2000 cm^{-1} indicating that the C_{2v} symmetry is retained. The IR spectra show that the reaction is highly selective, producing only the desired product since no other peaks due to byproducts are observed. IR is depicted in figure 3.18.

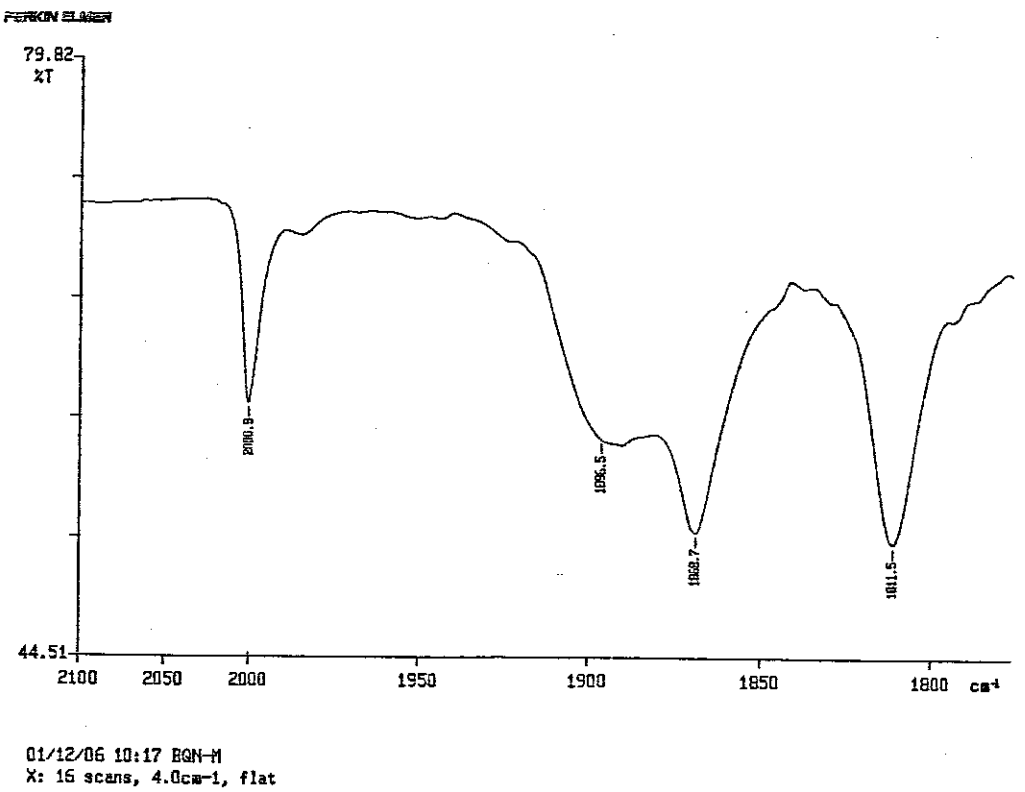

Figure 3.18_ IR for $[W(CO)_4bqn]$

3.2.6 UV-Visible Spectroscopy

The visible region the spectrum of, $[W(CO)_4BQN]$ in dichloromethane solution consists of one absorption which is absent in the spectrum of the free ligand. This lowest energy band in the 575 nm region is assigned to metal-to-ligand charge-transfer transition. Table 3.3 shows the data. UV-visible is shown in Figure 3.19

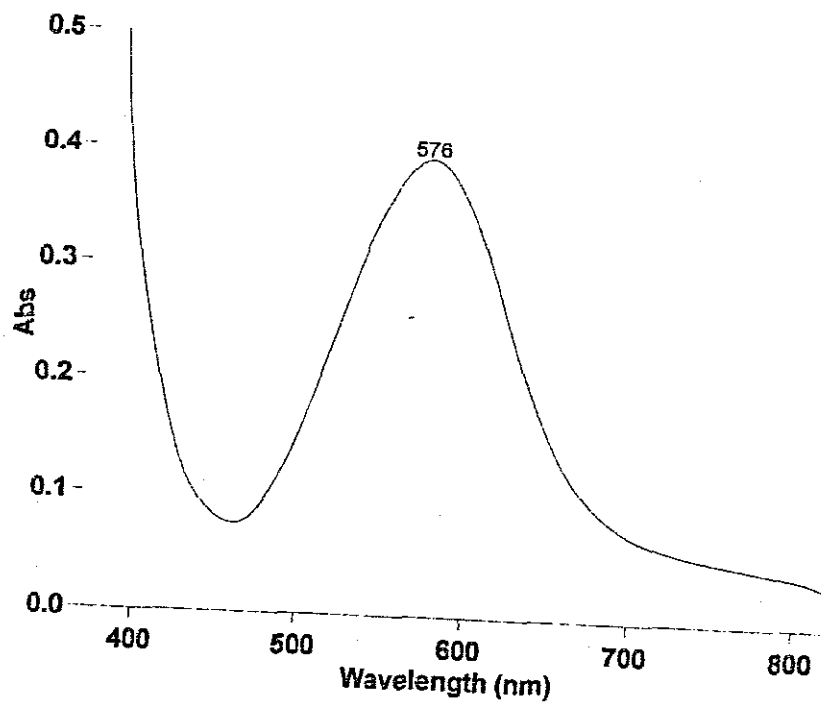

Figure 3.19_ UV-visible for $[W(CO)_4bqn]$

The absorption spectra of this complex show ligand centered band in the UV region and a broad metal-to-ligand charge- transfer band in the visible region.

3.2.6 Photoluminescence

This mononulear complex shows an emission band at 462 nm, which is assigned to MLCT. Figure 3.20 show the results

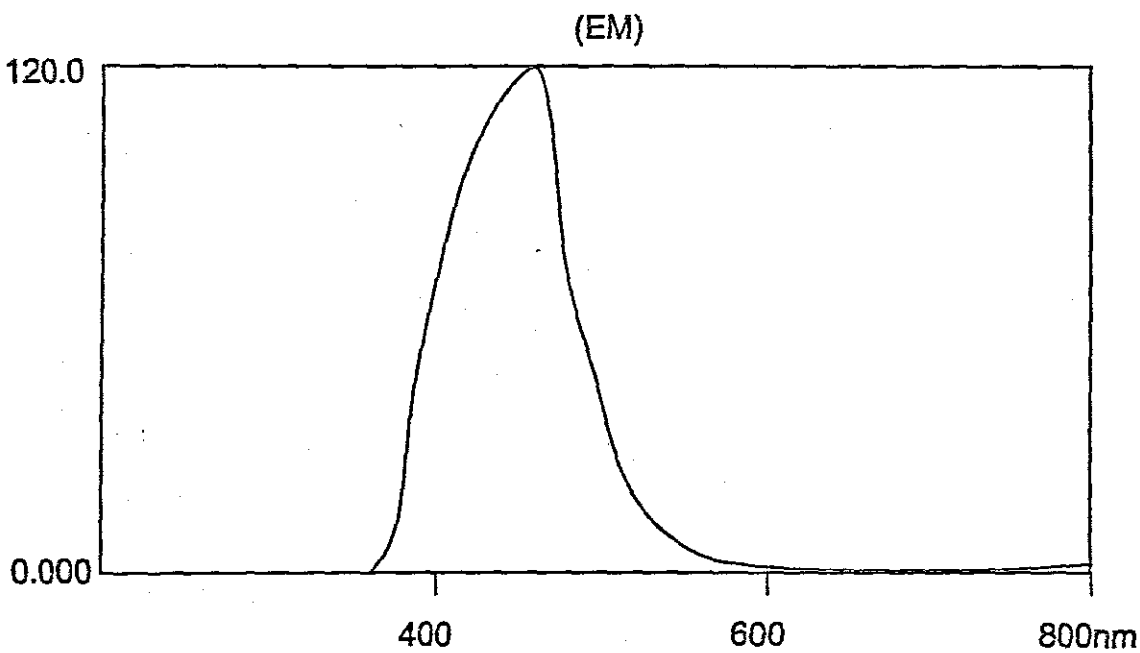

Figure 3.20_Emission spectra for $W(CO)_4$bqn

3.3. Tungsten complexes of 2,2-bipyrimidine

3.3.1 Synthesis of tetracarbonyl- 2,2`-bipyrimidinetungsten

The mononuclear complex has been reported using indirect substitution via $W(CO)_5THF$ adduct[16]. In this work direct photosubstitution of the ligand and tungsten hexacarbonyl was employed yielding the mononuclear and binuclear complex, which proves that this method is an appropriate and convenient method as compared to the earlier used by Chapman[66]. Equation for the reaction is indicated in the Scheme 3.3.

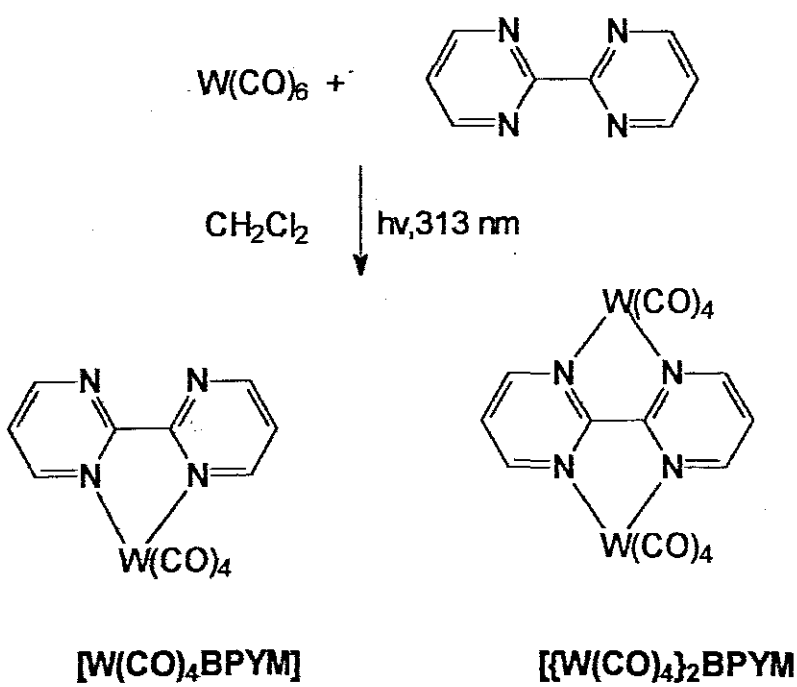

[W(CO)$_4$BPYM] [{W(CO)$_4$}$_2$BPYM

Scheme 3.3

Elution with CH_2Cl_2 gives the products in the order [$W(CO)_4$BPYM] and then [{$W(CO)_4$}$_2$BPYM]. The column chromatography gave two useful fractions. These complexes were found to be stable in solid form, but in solution are air and /or light sensitive with the dimer showing a greater proportion of decomposition. The instability of these complexes is thought to be due to cleavage of the M-L-M bond as shown in the bridged dimer [$(OC)_5Mo(pyz)Mo(CO)_5$][36]. More of the dimeric species was obtained by increasing the ratio of $W(CO)_6$. These complexes were characterized by a combination of IR, ^{1}H NMR and FAB mass spectroscopy, elemental analysis, cyclic voltammetry, photoluminescence and X-ray crystallography. The IR, ^{1}H NMR, CV, and PL for these complexes have not been reported.

3.3.2 Microanalysis, thin layer chromatography and Melting point

Sharp melting point, single spot on the thin layer chromatography and elemental analysis confirms the purity of the complexes where the binuclear complex, [{$W(CO)_4$}$_2$BPYM] showing lower melting point than the mononuclear , due to decomposition accompanied by evolution of CO. Microanalysis is shown in Table 3.1.

3.3.3 Infrared (IR) Spectroscopy

An infrared spectrum was recorded as KBr pellets. The infrared spectrum for the products showed that the carbonyl stretching peaks of the tungsten center adopts a C_{2v} symmetry and were consistent with *cis*-substituted tungsten tetracarbonyl complexes as only four bands are observed. These bands are assigned to A_1, B_1, A_1, and B_2 modes at 2004, 1904, 1864 and 1824 cm^{-1} for the $[W(CO)_4bpym]$ and 2005, 1919, 1889, and 1826 for the $[\{W(CO)_4\}_2bpym]$.

These vibrations are shown in Table 3.3. The IR is depicted in Figure 3.21

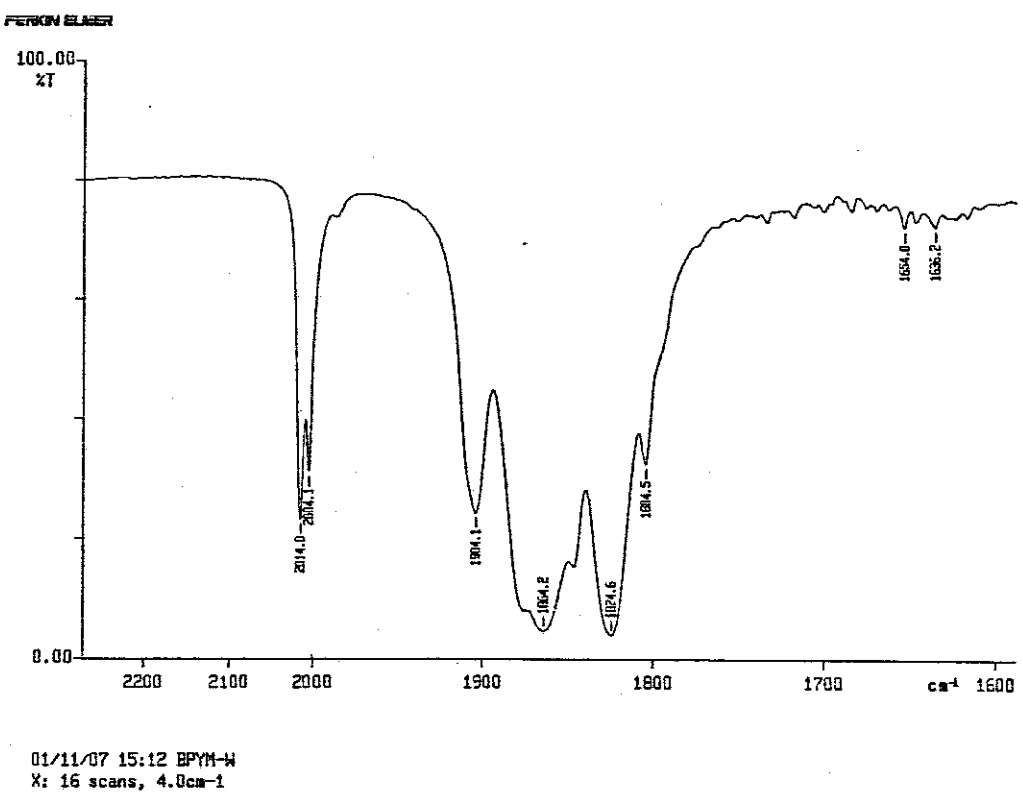

Figure 3.21_ IR spectra for $[W(CO)_4bpym]$

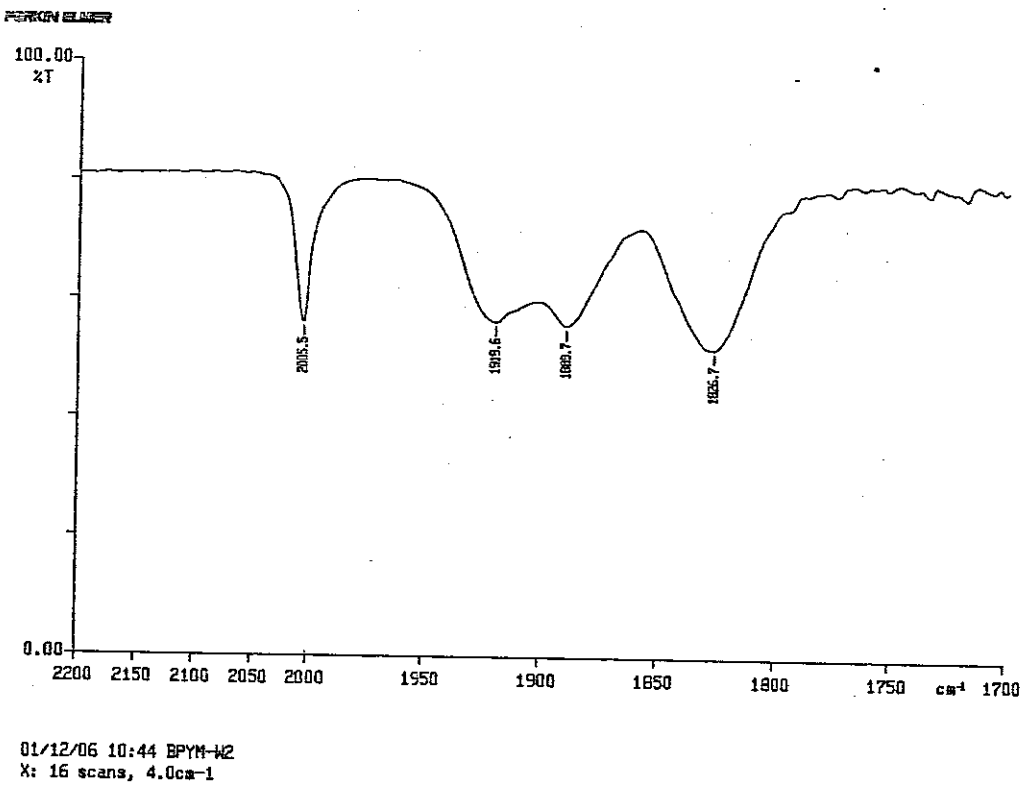

Figure 3.22_ IR spectrum of [{W(CO)$_4$}$_2$bpym]

3.3.4 UV-Visible Spectroscopy

When the BPYM ligand is bound to only one metal center, three bands are identified. The two bands at 300 and 379 nm near the UV region are assigned to intraligand transition. The lowest band in the visible region at 543 nm is associated with the MLCT transition.

When 2,2`-bipyrimidine (BPYM) ligand bridges two metal center, two absorption's bands, which are absent from the mononuclear, were observed. These absorptions are assigned to MLCT transition.

The formation of a binuclear system from the mononuclear fragment causes the MLCT bands to shift significantly toward lower energy. This is not surprising since the addition of electron withdrawing groups on the nitrogen heterocyclic (i.e. remote metal center) typically stabilizes the π system, thus reducing the energy of the π* orbital on the ligand and thus lowering the MLCT transition energy. Table 3.4 shows the results. Figures 3.23 and 3.24 show the results.

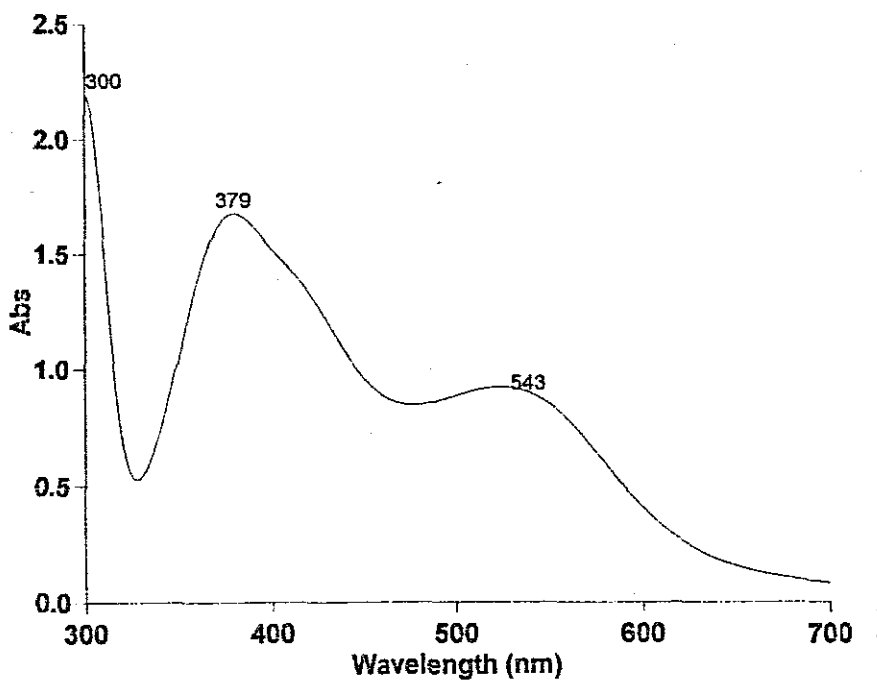

Figure 3.23 UV-visible for [W(CO)$_4$bpym]

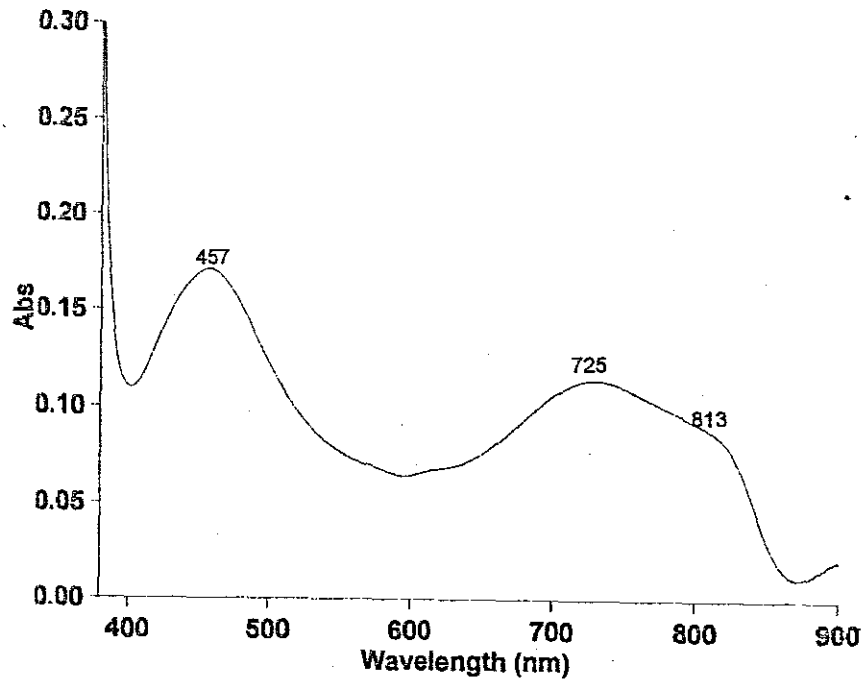

Figure 3.24_UV-visible for [{W(CO)$_4$}$_2$bpym

3.3.5 Photoluminescence

Three emissions were observed at 410 nm, 497 nm, and 597 nm for the mononuclear complex [W(CO)$_4$BPYM]. These emissions were assigned to MLCT transition. For the binuclear complex three emissions were observed at 327 nm, 494 nm, and 653 nm. Emission at 327 nm is assigned to $\pi \rightarrow \pi^*$ transition and the two emissions at 494 and 653 nm are assigned to MLCT. Figure 3.25 and 3.26 shows the results.

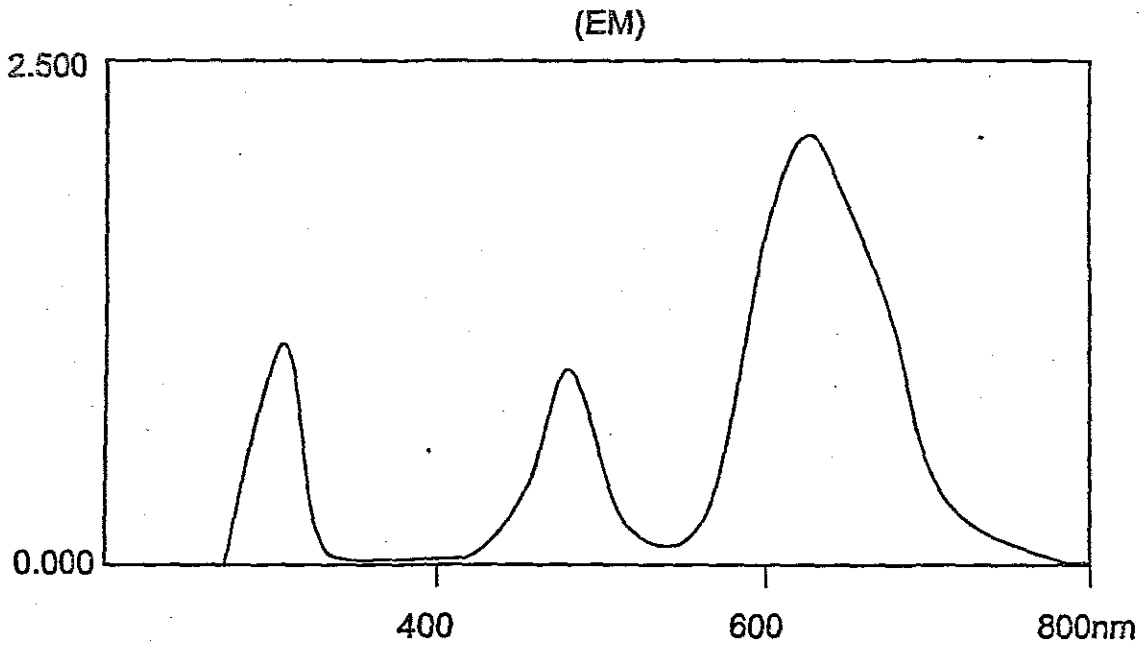

Figure 3.25_ Emission spectra for [W(CO)$_4$BPYM]

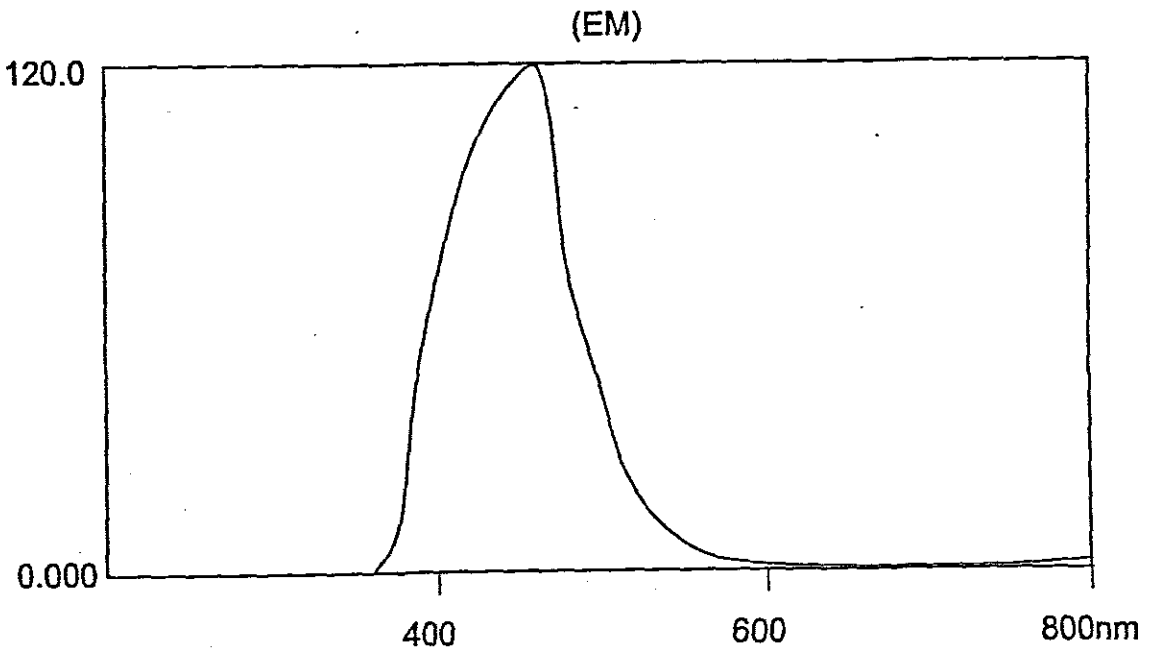

Figure 3.26_ Emission spectra for [{W(CO)$_4$}$_2$bpym]

3.4 Tungsten complex of tetracarbonyl-2,2`-bipyridine

3.4.1 Synthesis of tetracarbonyl 2,2`-bipyridinetungsten

Dichloromethane was used instead of hexane due to the low solubility in hexane of the starting materials. After 15-20 minutes a dark red crude product was obtained. Product purification was done using column chromatography on silica gel. Elution with pure dichloromethane leads to effective purification. The resulted complex has proved to be reasonably stable in solution. Equation of the reactions are shown below,

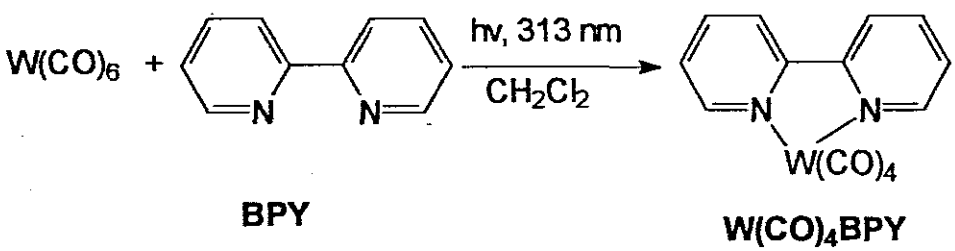

BPY **W(CO)$_4$BPY**

3.4.2 Microanalysis,Thin layer Chromatography and Melting point

Sharp melting point and thin layer chromatography confirm the purity of the mononuclear complex. Table 3.1 shows the results. Table 3.2 shows the microanalysis results.

3.4.3 Infrared spectroscopy

Infrared spectrum was recorded as KBr pellets. Four infrared-active CO stretching vibrational modes were obtained as expected for $[C_{14}H_8O_4N_2W]$, these being the $A_1(w)$,$B_1(st)$, $A_1(m)$ and $B_2(m)$. The four-carbonyl frequencies are closely related to those previously reported indicating that the local C_{2v} symmetry of $M(CO)_4$. The spectrum is depicted in Figure 3.27

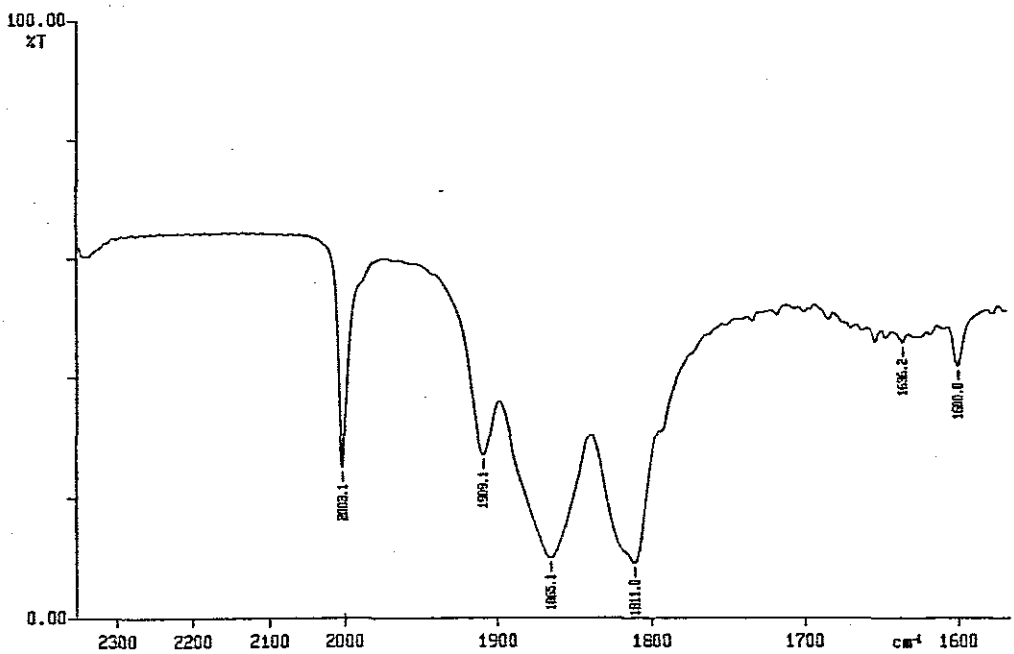

Figure 3.27_ IR for $[W(CO)_4bpy]$

3.4.4 UV-Visible spectroscopy

The UV-visible spectrum exhibits a sharp peak at 350 nm and a broader one at 485 nm. The lower energy transition is assigned to the W (0)→ BPY (π^*) metal-to-ligand charge-transfer transition. The band maximum at 350 nm is attributed to intraligand transition. The UV region is dominated by $\pi \rightarrow \pi^*$ transition of the bipyridine ligands, and the visible region consists of MLCT transition. Figure 3.28 shows the result.

Instrument Serial Number EL98013062

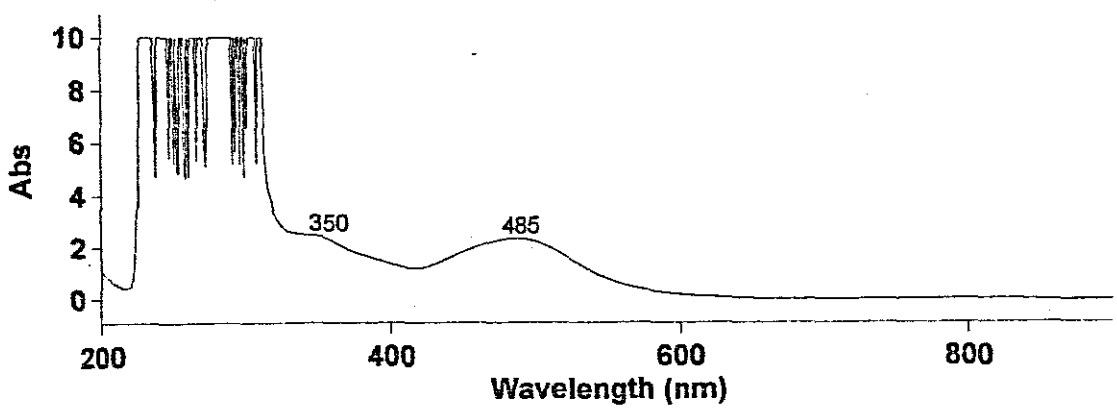

Figure 3.28_ UV-visible for [W(CO)$_4$bpy]

3.4.5 Photoluminescence

Three emission at 405 nm, 494 nm and 653 nm was observed which is assigned to MLCT.

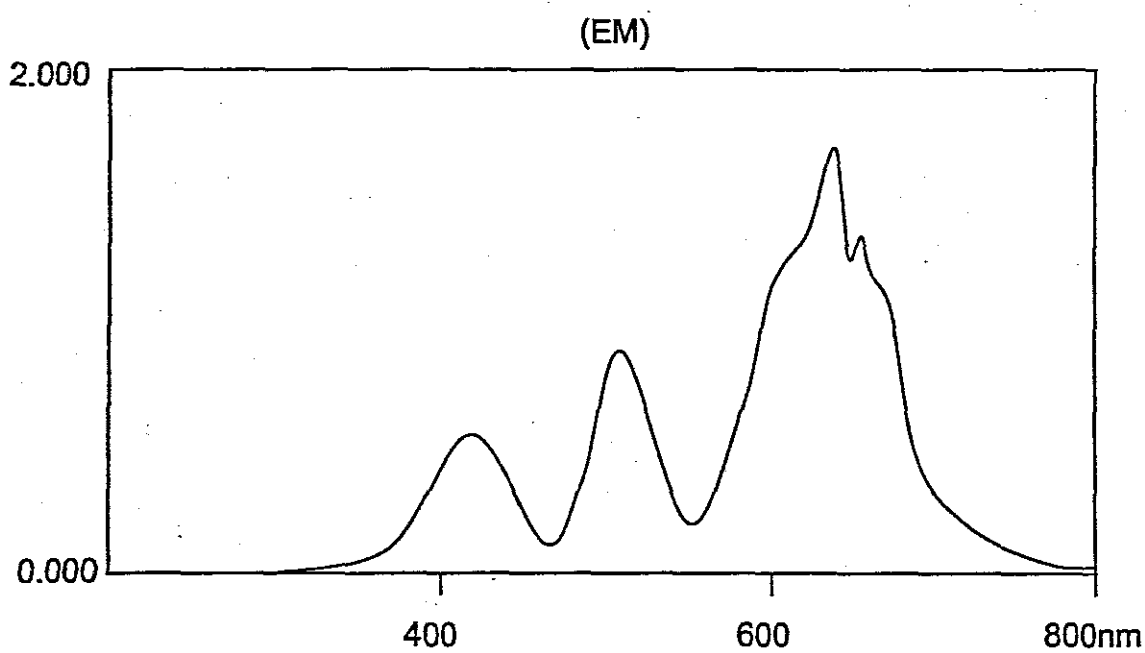

Figure 3.29_ Emission spectra for $[W(CO)_4bpy]$

3.4.6 Cyclic Voltammetry

Electrochemical behaviour of mononuclear tungsten complex shows the reduction potential at –2.230, -1.038, -0.626 and -0.928V. The voltammogram is depicted in figure 3.28.

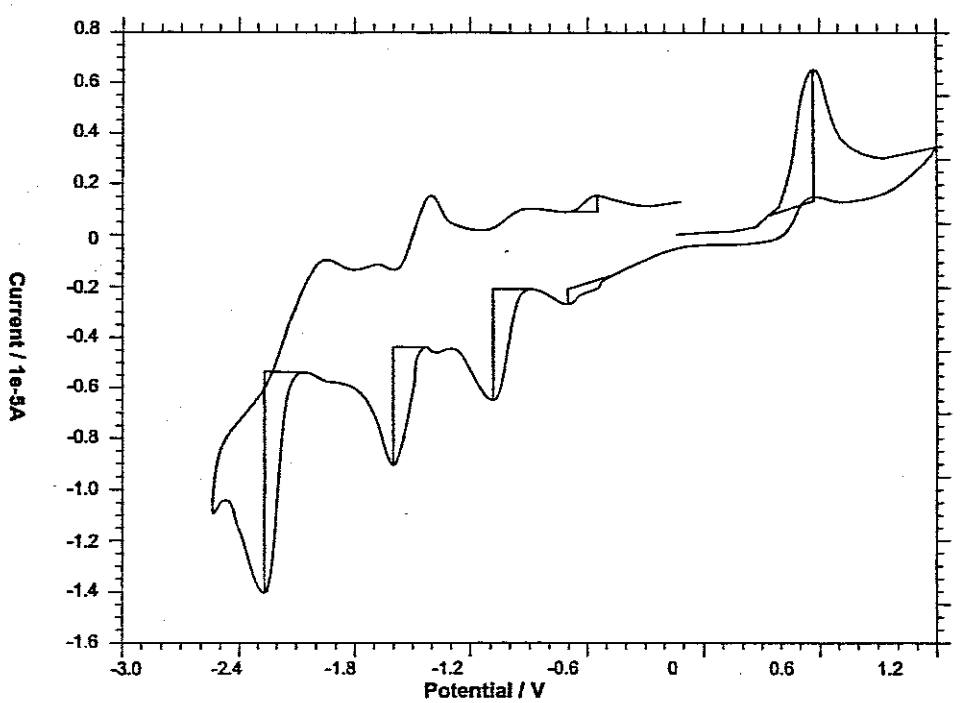

Figure 3.30 Redox potential of [W(CO)$_4$bpy]

Conclusion

We have investigated the physicalchemical properties of several organometallic complexes. Overall we have obtained interesting preliminary results for a variety of complexes, demonstrating the wide applicability of photochemistry. Organometallic photochemistry represents a rapidly expanding area of research due to the high efficiency and specificity possible *via* this route.

The stability of the complex depends on the metal and ligand present. Chromium complexes were found to be unstable in solution. The greater the number of metals presents, the lower the stability of the complexes, e.g. dimers are unstable in solution and have lower melting point. Synthetic procedure depends on the ligand e.g. unstable ligand show a higher degree of decomposition in polar solvents.

Infrared and UV-visible analyses of these complexes show that the reactions are highly selective, producing only the desired product since no peaks due to by- products are observed.

The fact that only desired products are formed in the reaction shows the highly systematic manner in which the complexes can be prepared unlike other synthetic methods.

Future studies

Using the knowledge and experience gained in this area, we hope to build and construct a range of metal conjugated organic systems, as dimers, oligomers and polymers. These novel complexes will be characterized with spectroscopic and physical measurements (i.e. electrochemical, conductometric and photochemical studies) and hopefully to identify possible technological application i.e. efficient conductors, solar energy harvesting technology.

Although the number of methods have been developed for the synthesis of organometallic dimers, oligomers, and polymers there is still a need for a way of generating complexes of defined length and metal content in systems where ring opening polymerization are appropriate.

We plan to synthesize a range of "building block'' ligand to form coordination compound with extended structures.

REFERENCES

1. E. Carol and R. P. Wayne, *Photochemistry* (1995), **39,** 85-86.
2. H. A. Cruse and N. E. Leadbeater, *Macromolecules*, (1999), **32,** 4450-4453
3. M.M Zulu and A.J. Lees, *Inorg. Chem*(1990),**29**,557-560
4. N.E. Leadbeater, *Inorg. Chimica Acta*(1998),**278**,250-252
5. G. L. Geoffroy, M. S. Wrighton, *Organometallic Photochemistry*, Academic Press, New York, (1979)
6. D.J. Darensbourg and M.A. Murphy, *Inorg. Chem.*(1978),**17**, 884-887
7. G.L. Geoffrey, *J.Chem. Ed.*,(1983), **60**, 861
8. D.R. Tyler, *J.Chem. Ed.*,(1997), **74**, 66
9. C. A. Hunter, *Angew.Chem, Int. Ed.Engl.* (1995), **34** ,1079-1081.
10. G. Shwenger, M. Y. Darensbourg, D. J. Darensbourg, *Inorg. Chem.* (1972), **11,** 1967-1970.
11. R. M. Dahlgren nad J. I. Zinc, *Inorg. Chem.* (1977), **16,** 3154-3156.
12. R. M. Dahlgren nad J. I. Zinc, *J. Am. Chem. Soc.* (1979), **101,** 1448.
13. J. E. Figard and J. D. Peterson, *Inorg. Chem.* (1979), **17,** 2736.
14. R. Ruminski and J. D. Peterson, *Inorg. Chem.* (1982), **21,** 3706-3708.
15. K. J. Moore, L. Lee, J. E. Figard, J. A. Gelroth, A. J. Stinson, H. D. Wohlers and J. D.Peterson, *J. Am. Chem. Soc.* (1983) , **105,** 2274-2279.
16. A. Nel, J. Chapman, N. Long, G.A. Kolawole, M Motevalli and P. O'Brien, *Polyhedron*(2000),**000**, 1-6

17. L. E. Orgel, *Inorg. Chem.*(1962), **1** , 25-28.

18. N.E. Leadbeater and H.A. Cruse, *Inorg. Chem.Comm*(1999),**2**, 93-94

19. G. Hogarth and T. Norman, *Polyhedron*, (1996),**15**, 2859

20. E. Waldhor, M.M. Zulu, S. Zalis and W.Kaim, *J.Chem. Soc., Perkin Trans.2* (1996), 1197-1203.

21. W. Kaim, S. Ernst and S. Kohlman, *Polyhedron*(1986),**5**, 445-449

22. M.Y. Darensbourg, and D.J. Darensbourg, *Journal of chemical Education*(1974),**51**,787-789.

23. J. K. Farr, L. G. Hulett, R. H Lane and J. K. Hurst, *J. Am. Chem. Soc.* (1975), **97**, 2654.

24. V. A. Durant and P. C. Ford, *J. Am. Chem. Soc.* (1975), **97**, 6898. D. A. Piering and J. M. Malin, *J. Am. Chem. Soc.*, (1976), **98**, 6043.

25. K. S. Schanse, G. A. Neyharf and T. J. Meyer, *J.Phys.chem.* (1986), **90**, 2182-2193.

26. J. A. Gelroth, J. E. Figard, J. D. Peterson, *J. Am. Chem. Soc.* (1979), **101**, 3649-3650.

27. J. D. Peterson, W. R. Murphy, R. Sahai, K. J. Brewer, and R. R. Ruminski, *Coord. Chem. Rev.* (1985), **64**, 261-272.

28. W. L. Bowden , W. F. Little, T. J. Meyer, D. Salmon , *J. Am. Chem. Soc.* (1975), 6899.

29. A. J. Lees , J. M. Fobare and E. F Mattimore, *Inorg. Chem.* (1984), **23**, 2709-2713.

30. N.J. Long, *Angew.Chem.(Int.Ed.Engl.)*,(1995), **34**, 21

31. M. M. Zulu and A. J. Lees*, *Inorg. Chem.* (1989), **28,** 85-89.

32. L. Mukerjee, S.P. Nolan, C.D. Hoff and R.L. de lavega, *Inorg.Chem* (1988), **27**, 81-85

33. Barigelleti, L. Decola, V. Balzani, R. Hage, J.G. Haasnoot, *Inorg. Chem* (1989), **28**, 4344-4350

34. H. Saito, J. Fujiita, K. Saito, *Bull.Chem.Soc.Jpn.*(1968), **41**, 863-874

35. C. Overton and J.A. connor, *Polyhedron* (1982),**1**, 53-56.

36. A. Nel, J.Chapman, N.Long, G. Kolawole, M.Motevalli, and P.O`brien, *Polyhedron,*(2000), **19**,1621

37. M.Y. Darensbourg, and D.J. Darensbourg, *Journal of chemical Education*(1970),**47**,33-35.

38. D.M. Manuta and A.J. Lees, *Inorg. Chem*(1983),**22**, 3825-3828

39. S. Ernst and W. Kaim, *J. Am.Chem.Soc.*(1986), **108**, 3578-3586

40. A.Das, J.P. Mahor, J.A McCleverty, J.A. Badiola and M.D Ward, *J. Chem. Soc. Dalton Trans* (1993), 681-686.

41. S.Kohlmann, S. Ernst and W Kaim, *Angew. Chem.Int. Ed. Engl.* (1985), **24**, 684-685.

42. J. Studebaker, R. Srinivasan, J.A. Ors and T.Baum, *J.Am. Chem. Soc.*(1980), **102**, 6874-6876

43. M.M. Zulu and A.J. Lees*, *Inorg. Chem.* (1988), **27**, 1139-1145.

44. R.J. Dennenberg and D.J. Darensbourg, *Inorg. Chem.* (1972), 11, 72-77.

45. E.V. Dose, L.J. Wilson, *Inorg. Chem.* (1978), **17**, 2660

46. M. Hunziker, A. Ludi, *J. Am. Chem. Soc.*(1977), **99**,7370

47. W. Kaim, and S. Kohlmann, *Inorg. Chem.* (1990), **29**,2909-2914.

48. E.C. Alyea, J. Malito, S.D. Ernst, W. Kaim and S.J. Kohlmann, *Polyhedron* (1989),**8**, 921-924.

49. M.M. Zulu and A.J. Lees*, *Inorg. Chem.* (1988), **27**, 3325-3327.

50. M.M. Zulu, and A.J. Lees, *Organometallics* (1989), **8**, 955-960.

51. W.L Jolly, *Syn. And charact. Of Inorg. Compounds*

52. A.J. Blake, N.R. Champness, P. Hubbersley, W.S. Li, M.A. Witherby, and M. Schroder, *Coord. Chem.Rev.*, (1999),**183**, 17

53. F. S. Campagna, G. Denti, G. De rosa, L. Sabatino, M. Ciano, and V. Balzani, *Inorg. Chem* (1989), **28**, 2565-2570

54. G. Malouf, and P.C. Ford, *J.Am. Chem. Soc.*(1977), **96**, 601

55. R.Hage, A.H.J Dijkhuis, J.G. Haasnoot, R. Prins, J. Reedijk, B.E. Buchanan, and J.G. Vos, *Inorg. Chem*(1988), **27**, 2185-2189

56. D. Rillema, and K.B. Mack, *Inorg.Chem*(1982), **21**, 3849-3854

57. Q. Jaradat, K. Barqawi and T.S Akashett, *Inorgonica Chimica Acta*(1986),**116**, 63-73.

58. E. Waldhor, M.M. Zulu, S. Zalis and W.Kaim, *J.Chem. Soc., Perkin Trans.2* (1996), 1197-1203.

59. G. Boxhoorn, A. oskam, E.P. Gibson, R. Narayanaswamy and A.J. Rest, *Inorg.Chem*(1981),**20**, 783-786

60. G. Boxhoorn, G.C. Schoemaker, D.J. Stufkens, A. Oskam, A.J. Rest and D.J. Darensbourg. *Inorg. Chem*(1980),**19**, 3455-3461

61. M.S. Wrighton and D.L Morse, *J.Organo. Chem*,(1975),**97**, 405-420

62. S.R. Battern and R.Robson, *Angew.Chem.(Int.Ed. Engl)*,(1998), **37**,1460

63. L. Dai, Z. Zhou, Y-Zhang, C. Ni, Z. Zhang and Y. Zhou, *J.Chem.Soc., Chem. Commun.*,(1987),1760-1762.

64. R. Uson, J. Fornies, M. Tomas, J.M. Casas and C. Fostuno, *Polyhedron* (1989), **8**, 2209-2211.

65. K.J. Brewer, W. Murphy, Jr., and J.D Peterson, *Inorg. Chem.* (1987),**26**, 3376-3379

66. J Chapman, unpublished data.